

105, Rev. A

Atmospheric and Environmental Effects

December 15, 2002

Prepared by:

S.D. Slobin 12-9-02

S. D. Slobin,
Antenna System Engineer

Date

Approved by:

A. J. Freiley 12-9-02

A. J. Freiley
Antenna Product Domain Service
System Development Engineer

Date

Released by:

[Signature on File]
at DSMS Library

2/10/03

DSMS Document Release

Date

Change Log

Rev	Issue Date	Affected Paragraphs	Change Summary
Initial	11/30/2000	All	All
A	12/15/2002	All	Provides monthly weather statistics for all stations and frequency bands

Note to Readers

There are two sets of document histories in the 810-005 document that are reflected in the header at the top of the page. First, the overall document is periodically released as a revision when major changes affect a majority of the modules. For example, this document is part of Revision E. Second, the individual modules also change, starting as the initial issue that has no revision letter. When a module is changed, a change letter is appended to the module number on the second line of the header and a summary of the changes is entered in the module's change log.

Contents

<u>Paragraph</u>		<u>Page</u>
1	Introduction.....	6
1.1	Purpose	6
1.2	Scope	6
2	General Information	7
2.1	Atmospheric Attenuation and Noise Temperature.....	7
2.1.1	Calculation of Mean Atmospheric Physical Temperature.....	10
2.1.2	Elevation Angle Modeling.....	10
2.1.3	Calculation of Noise Temperature From Attenuation	10
2.1.4	Cosmic Background Adjustment.....	11
2.1.5	Example of Use of Attenuation Statistics to Calculate Atmospheric Noise Temperature, $T_{atm}(\theta, CD)$, and $T_{op}(\theta, CD)$	12
2.1.6	Best/Worst Month Ranges of Atmospheric Noise Temperature and Attenuation.....	12
2.2	Rainfall Statistics.....	13
2.3	Wind Loading.....	14
2.4	Hot Body Noise.....	14
2.4.1	Solar Noise.....	14
2.4.2	Lunar Noise.....	17
2.4.3	Planetary Noise	18
2.4.4	Galactic Noise	19

Illustrations

<u>Figure</u>		<u>Page</u>
1.	Cumulative Distributions of Zenith Atmospheric Noise Temperature at L-Band and S-Band, Goldstone DSCC	20
2.	Cumulative Distributions of Zenith Atmospheric Noise Temperature at L-Band and S-Band, Canberra DSCC.....	21
3.	Cumulative Distributions of Zenith Atmospheric Noise Temperature at L-Band and S-Band, Madrid DSCC	22
4.	Cumulative Distributions of Zenith Atmospheric Noise Temperature at X-Band, Goldstone DSCC.....	23

5.	Cumulative Distributions of Zenith Atmospheric Noise Temperature at X-Band, Canberra DSCC.....	24
6.	Cumulative Distributions of Zenith Atmospheric Noise Temperature at X-Band, Madrid DSCC	25
7.	Cumulative Distributions of Zenith Atmospheric Noise Temperature at Ka-Band, Goldstone DSCC.....	26
8.	Cumulative Distributions of Zenith Atmospheric Noise Temperature at Ka-Band, Canberra DSCC.....	27
9.	Cumulative Distributions of Zenith Atmospheric Noise Temperature at Ka-Band, Madrid DSCC	28
10.	Probability Distribution of Wind Conditions at Goldstone.....	29
11.	Solar Radio Flux at 2800 MHz (10.7 cm wavelength) During Solar Cycle 23 (1996–2007).....	30
12.	DSS 15 HEF Antenna X-Band System Noise Temperature Increases Due to the Sun at Various Offset Angles, Showing Larger Increases Perpendicular to Quadripod Directions	31
13.	DSS 16 S-Band Total System Noise Temperature at Various Offset Angles from the Sun.....	32
14.	DSS 12 S-Band Total System Noise Temperature at Various Declination and Cross-Declination Offsets from the Sun.....	33
15.	DSS 12 X-Band Total System Noise Temperature at Various Declination and Cross-Declination Offsets from the Sun.....	34
16.	DSS 13 Beam-Waveguide Antenna X-Band Noise Temperature Increase Versus Offset Angle, March 1996	35
17.	DSS 13 Beam-Waveguide Antenna Ka-Band Noise Temperature Increase Versus Offset Angle, March 1996	35
18.	Total S-Band System Noise Temperature for 70-m Antennas Tracking Spacecraft Near the Sun (Derived from 64-m Measurements)	36
19.	X-Band Noise Temperature Increase for 70-m Antennas as a Function of Sun-Earth-Probe Angle, Nominal Sun, 23,000 K Disk Temperature	37

Tables

<u>Table</u>	<u>Page</u>
1. Cumulative Distributions of Zenith Atmospheric Noise Temperature at L- and S-Bands for Goldstone DS ^C C.....	38
2. Cumulative Distributions of Zenith Atmospheric Noise Temperature at L- and S-Bands for Canberra DS ^C C	39
3. Cumulative Distributions of Zenith Atmospheric Noise Temperature at L- and S-Bands for Madrid DS ^C C	40
4. Cumulative Distributions of Zenith Atmospheric Noise Temperature at X-Band for Goldstone DS ^C C.....	41
5. Cumulative Distributions of Zenith Atmospheric Noise Temperature at X-Band for Canberra DS ^C C	42
6. Cumulative Distributions of Zenith Atmospheric Noise Temperature at X-Band for Madrid DS ^C C	43
7. Cumulative Distributions of Zenith Atmospheric Noise Temperature at Ka-Band for Goldstone DS ^C C.....	44
8. Cumulative Distributions of Zenith Atmospheric Noise Temperature at Ka-Band for Canberra DS ^C C	45
9. Cumulative Distributions of Zenith Atmospheric Noise Temperature at Ka-Band for Madrid DS ^C C	46
10. Cumulative Distributions of Zenith Atmospheric Attenuation at L- and S-Bands for Goldstone DS ^C C.....	47
11. Cumulative Distributions of Zenith Atmospheric Attenuation at L- and S-Bands for Canberra DS ^C C	48
12. Cumulative Distributions of Zenith Atmospheric Attenuation at L- and S-Bands for Madrid DS ^C C	49
13. Cumulative Distributions of Zenith Atmospheric Attenuation at X-Band for Goldstone DS ^C C	50
14. Cumulative Distributions of Zenith Atmospheric Attenuation at X-Band for Canberra DS ^C C.....	51
15. Cumulative Distributions of Zenith Atmospheric Attenuation at X-Band for Madrid DS ^C C.....	52
16. Cumulative Distributions of Zenith Atmospheric Attenuation at Ka-Band for Goldstone DS ^C C	53

17. Cumulative Distributions of Zenith Atmospheric Attenuation at Ka-Band for Canberra DSCC.....	54
18. Cumulative Distributions of Zenith Atmospheric Attenuation at Ka-Band for Madrid DSCC.....	55
19. Monthly and Year-Average Rainfall Amounts at the DSN Antenna Locations.....	56
20. Parameters for X-Band Planetary Noise Calculation, plus X-Band and Ka-Band Noise Temperatures at Mean Minimum Distance from Earth.....	57

1 *Introduction*

1.1 *Purpose*

This module provides sufficient information concerning atmospheric, environmental, and extraterrestrial effects to enable a flight project to design a telecommunications link at the L-, S-, X, and Ka-band frequencies used by the DSN.

1.2 *Scope*

Statistics of atmospheric attenuation and noise temperature at each tracking antenna site are presented for those microwave frequencies used by the DSN. In this module, the values of attenuation and noise temperature increase are given relative to a no-atmosphere (vacuum) condition thus, this presentation is compatible for use with the vacuum gain and noise temperature presentations of antenna performance given in modules 101 for 70-m antennas, 102 for 26-m antennas, 103 for 34-m high-efficiency (HEF) antennas, and 104 for 34-m beam-waveguide (BWG) antennas.

Statistics of wind speed at Goldstone are given. These are used both to determine the statistics of antenna gain reduction due to wind loading and also to ascertain the percentage of time an antenna will be unusable due to excessive wind speed.

Extraterrestrial effects are primarily the increased system noise temperature due to hot body noise from the Sun, Moon, planets, and galactic radio sources. These effects are significant only when the antenna beam is in the vicinity of these noise sources during tracking of spacecraft.

Charged-particle effects are given in module 106, Solar Corona and Solar Wind Effects.

2 *General Information*

2.1 *Atmospheric Attenuation and Noise Temperature*

The principal sources of atmospheric attenuation and noise temperature weather effects are oxygen, water vapor, clouds, and rain. These two effects are related, and higher atmospheric attenuation produces a higher noise contribution. Also, atmospheric effects generally increase with increasing frequency. Ka-band effects are larger than X-band effects, which are larger than S-band and L-band effects.

In the 810-005 antenna performance modules (modules 101, 102, 103, and 104), *effective antenna gain* (vacuum gain minus atmospheric attenuation) is presented in the figures for various atmospheric attenuation values. Strictly speaking, the gain of an antenna is not a function of atmospheric attenuation; however for stand-alone use, the effective gain, including atmospheric loss, is a useful concept, and the expressions for gain in the appendices of those modules include a term for atmospheric attenuation. Similarly, system operating noise temperature as presented in the appendices of those modules also includes a term for atmospheric noise contribution, although the *antenna temperature* (due to spillover, LNA contribution, waveguide loss, etc.) is also not a function of atmosphere contribution. The vacuum system noise temperature as given in those modules includes the nearly constant contribution from the cosmic background, which adds to the basic antenna temperature value.

Design control tables used for telecommunications link design typically carry separate entries for atmospheric attenuation of the received or transmitted signal and atmospheric noise contribution as a function of elevation angle and weather condition. It is important in those DCTs that the antenna gain and system operating noise temperature values reflect the vacuum performance of the antenna, so as to prevent double-bookkeeping of the atmospheric attenuation and noise temperature contributions.

The atmospheric models presented here give L-band (1.7 GHz), S-band (2.3 GHz), X-band (8.4 GHz), and Ka-band (32.0 GHz) atmospheric noise temperature and attenuation statistics in the form of cumulative distributions (CDs) for each effect. A cumulative distribution of 0.90 (90% weather) means that 90% of the time a particular weather effect (noise temperature or attenuation) is less than or equal to a given value. Conversely, that particular effect is exceeded only 10% of the time. Qualitatively, the weather conditions associated with selected cumulative distributions are described as follows:

CD = 0.00	clear dry, lowest weather effect
CD = 0.25	average clear weather
CD = 0.50	clear humid, or very light clouds
CD = 0.90	very cloudy, no rain
CD > 0.95	very cloudy, rain

By their very natures, clouds and rain are poorly modeled, and the water vapor radiometer data used here are sparse for the larger weather effects, which are exceeded only 5% of the time.

The Ka-band model presented here is based on actual water vapor radiometer noise temperature measurements made at 31.4 GHz at all three DSN sites (Goldstone, Canberra, and Madrid). Used in the modeling were 66 months of Goldstone data covering the period October 1993 through August 2002, 35 months of Canberra data covering the period June 1999 through August 2002, and 112 months of Madrid data covering the period September 1990 through August 2002. There were missing months of data from each station. Note also that different numbers of months of data went into the model for each of the separate months (e.g., there may have been 6 Februaries, but only 4 Marches). It is felt that because of the large amount of Madrid data (more than 9 years), the results will fairly accurately represent true long-term statistics. The 5-1/2 years of Goldstone data will give a moderately accurate long-term model. The three years of Canberra data will probably not give a very accurate long-term model, and future updates of the Canberra model are likely to show relatively large changes in the distributions. Cumulative distributions at 31.4 GHz for each of the 12 months were calculated, then increased by 0.3 K (the oxygen-only difference due to frequency) to create a model for 32 GHz. A year-average model was developed by calculating the average noise temperature of all the 12 months, at each CD level.

L-/S-band and X-band statistics were created from the Ka-band (32 GHz) statistics by subtracting out the 0% CD baseline (calculated for nominal temperatures and pressures, with 0% relative humidity), frequency squaring to the appropriate frequency (for example, $[8.42/32.0]^2$) and then adding in the 0% CD baseline at the new frequency. Note that the 0% CD baselines for the DSN sites differ because of different heights above sea level.

Atmospheric attenuation statistics were created from the noise temperature statistics by methods given in Sections 2.1.1 and 2.1.3 below. The year-average attenuation statistics were calculated from the year-average noise temperature values rather than by calculating the average of all the monthly attenuations. These two methods give very slightly different results.

It should be noted that although the noise temperature statistics are the best qualitative measures for comparison of different locations and different frequencies, especially when dealing with low-noise systems (where the atmospheric noise is a large part of the total system noise temperature), the basic data base of atmospheric effects is actually the attenuation statistics. Given a station location, frequency, and CD of interest, the attenuation data base value is extracted, modeled to the elevation angle of interest (Section 2.1.2), and then the appropriate atmospheric noise temperature is calculated (Section 2.1.3). In this way, the original zenith noise temperature statistics (Tables 1 through 9) can be re-calculated from the zenith attenuation values (Tables 10 through 18) using the method given in Section 2.1.3.

The atmospheric models thus generated for a particular complex (for example, Goldstone) should be used for all antennas at that complex (for example, DSS 14, DSS 15, DSS 24, etc.), regardless of the small altitude differences among the antennas.

Zenith atmospheric noise temperature statistics for the three DSN sites at S-band are provided in Tables 1 through 3. Tables 4 through 6 provide similar statistics for X-band and Tables 7 through 9 cover Ka-band. The tables include the maximum and minimum value for each CD level, the year average for that CD level and the average value for each month. These noise temperature statistics should be used only in a qualitative sense to describe the relative levels of atmospheric noise contributions at different locations and cumulative distributions. They should not be used for elevation modeling as this is properly performed using the calculated attenuation at a given elevation angle as a starting point and following the process that is described below.

The use of these statistics depends on the context in which the antenna temperature is stated. When a nominal antenna zenith T_{op} (operating system noise temperature) is stated, it is considered to include the CD = 25% (average clear sky) value for the appropriate frequency and location. However, “vacuum” antenna temperatures are sometimes used to describe the performance of an antenna independent of location. In this case the operating system noise temperature should be referred to as $T_{op, vac}$.

Tables 10 through 18 provide similar presentations for zenith atmospheric attenuation. It can be noted that the L-/S-band attenuations do not monotonically increase as a function of CD, whereas the corresponding noise temperatures do. This is an artifact of the relationship between the modeled mean physical temperature of the atmosphere and the noise temperature used to calculate the corresponding attenuation. This relationship is seen below. In any case, the atmospheric effect at L-/S-band is nearly constant (to within 0.1 K and 0.003 dB over the CD range from 0% to 90%), and this small anomaly does not contribute to significant errors in modeling telecommunications performance.

The tolerances of atmospheric noise temperature and attenuation, as given in Tables 1 through 18, should be considered to be 5% of the stated values at zenith, or 5% of the values calculated for elevation angles other than zenith. (see Section 2.1.5, below).

Figures 1, 2, and 3 show the L-/S-band noise temperature statistics for Goldstone, Canberra, and Madrid respectively. Figures 4, 5, and 6 show X-band statistics for the three complexes. Figures 7, 8, and 9 provide the Ka-band statistics. On each figure, the year-average cumulative distribution, the minimum envelope value, and the maximum envelope values are given for all the individual months at each CD value stated in Tables 1–9. The year-average model from the previous revision of module 105 (dated November 30, 2000) is also given to aid the user in assessing the changes from one model to the next. Curves of zenith attenuation are not given, although using a rule-of-thumb that a medium with 1 dB attenuation radiates a noise temperature of approximately 60 K, the Ka-band curves can be used to make rough estimates of the zenith attenuation at the various frequencies. This relationship is nearly linear over the range from 0 to 1 dB.

For Ka-band, using 90% CD as a reference point, it is seen qualitatively that the Goldstone year-average model shows better weather than the previous module 105 presented; Canberra shows identical weather, although better at higher CDs; and Madrid slightly worse at 90% and slightly better above 96%.

For other nearby frequencies within the L-, S-, X-, and Ka-bands, the weather-effects models presented here should be used without modification.

2.1.1 *Calculation of Mean Atmospheric Physical Temperature*

The mean physical temperature of the atmosphere is modeled to be a function of weather condition, or cumulative distribution. This reflects the assumption that those effects that are of larger value (for example, high noise temperature) occur closer to the surface and hence are at a higher average physical temperature than those that have a lesser effect. The mean atmospheric physical temperature is modeled as

$$T_p = 255 + 25 \times CD, \text{ K} \quad (1)$$

where

CD = cumulative distribution of weather effect ($0.0 \leq CD \leq 0.99$).

Note that the maximum value of T_p thus becomes nearly 280 K.

2.1.2 *Elevation Angle Modeling*

Only the attenuation should be modeled as a function of elevation angle. The atmospheric noise temperature contribution at any elevation angle can be calculated from the modeled attenuation at that elevation angle. Elevation angle modeling can be performed using either a flat-Earth or a round-Earth model. A flat-Earth model is used here, wherein the attenuation increases with decreasing elevation angle:

$$A(\theta) = A_{zen} \times AM = \frac{A_{zen}}{\sin(\theta)}, \text{ dB} \quad (2)$$

where

θ = elevation angle of antenna beam

A_{zen} = zenith atmospheric attenuation (dB), as given in Tables 10 through 18

AM = number of air masses (1.0 at zenith)

The flat-Earth approximation produces a slightly higher attenuation than would be obtained with a round-Earth model for low elevation angles but is valid to within 1% to 3% at a 6-deg elevation angle, depending on the frequency and the amount of water vapor in the atmosphere.

2.1.3 *Calculation of Noise Temperature From Attenuation*

An attenuating atmosphere creates a noise temperature contribution to ground antenna system temperature. The atmospheric noise temperature at any elevation angle (θ) is calculated from the attenuation by

$$T_{atm}(\theta) = T_p \left[1 - \frac{1}{L(\theta)} \right], \text{ K} \quad (3)$$

where

$$\begin{aligned} T_p &= \text{mean physical temperature of atmosphere (K), calculated above} \\ L(\theta) &= \text{loss factor of atmosphere} = 10^{\left[\frac{A(\theta)}{10} \right]} \\ A(\theta) &= \text{atmospheric attenuation at any elevation angle (dB), calculated above} \end{aligned}$$

Note that typical values of L range from about 1.01 to 2.0

2.1.4 *Cosmic Background Adjustment*

The noise temperature contribution of the cosmic background is reduced by atmospheric attenuation. For the bands of interest, the effective cosmic background noise before atmospheric attenuation is

$$\begin{aligned} T_c &= 2.7 && (\text{L-band and S-band}) \\ &= 2.5 && (\text{X-band}) \\ &= 2.0 && (\text{Ka-band}) \end{aligned}$$

With atmosphere, the effective cosmic background effect is

$$T'_c(\theta) = \frac{T_c}{L(\theta)}, \text{ K} \quad (4)$$

where

$$\begin{aligned} T_c &= \text{effective cosmic background noise (K) without atmosphere} \\ L(\theta) &= \text{loss factor of atmosphere at the elevation angle of interest, as calculated from Section 2.1.3.} \end{aligned}$$

The expressions for $T_{op, vac}$ in the telecommunications interface modules (for example, module 101) include the effective cosmic background contribution reduced by the effects of average clear weather. These values are within a few tenths of a Kelvin of the values given above, and variations in T'_c as a function of weather condition and elevation angle are typically neglected, as being at the sub-1K level.

2.1.5

Example of Use of Attenuation Statistics to Calculate Atmospheric Noise Temperature, $T_{atm}(\theta, CD)$, and $T_{op}(\theta, CD)$

The following example will show a typical calculation of atmospheric noise temperature and attenuation for a particular situation. The parameters for the example are

DSS 43, Canberra

Ka-band (32 GHz)

90% year average weather (CD = 0.90)

20-deg elevation angle (2.924 air masses)

From Table 17, the year average zenith attenuation is given as

$$A_{zen} = 0.404 \text{ dB.}$$

The attenuation at 20-deg elevation is

$$A(20^\circ, 90\%) = \frac{0.404}{\sin(20)} = 1.181 \text{ dB}$$

The loss factor L at 20-deg elevation is

$$L(20^\circ, 90\%) = 10^{0.1181} = 1.312$$

The atmospheric mean physical temperature is

$$T_p = 255 + 25 \times 0.90 = 277.5 \text{ K}$$

The atmospheric noise temperature at 20-deg elevation is

$$T_{atm}(20^\circ, 90\%) = 277.5 \left(1 - \frac{1}{1.312}\right) = 65.991 \text{ K}$$

The operating system noise temperature at any elevation angle and for any weather condition is given by

$$T_{op}(\theta, CD) = T_{op, vac}(\theta) + T_{atm}(\theta, CD), \text{ K} \quad (5)$$

where

$T_{op, vac}(\theta)$ = vacuum system temperature at elevation angle θ from the appropriate antenna performance module (101, 102, 103 or 104).

2.1.6

Best/Worst Month Ranges of Atmospheric Noise Temperature and Attenuation

Although the absolute accuracy of the 31.4-GHz water vapor radiometer measurements used to create the noise temperature statistics is thought to be on the order of the values stated in paragraph 2.1, the month-to-month variation of average noise temperature at any

CD varies much more than this at all values of cumulative distribution greater than about 10%. A particular month might be the "worst" at the 90% CD level, but merely "moderate" at lower CD levels. An example is a winter month that has a large amount of rain but when not raining has low humidity and low noise temperature contribution. At this time, there are insufficient data to characterize "best" and "worst" months individually; however, tolerances on the mean statistics as given in Tables 1 through 18 can give the user a feeling of what yearly variations in atmospheric effects may be expected.

Inspection of Tables 1 through 18 and Figures 1 through 9 will show that fictitious "best month" and "worst month" statistics can be generated from the values giving the minimum and maximum envelope values of noise temperature and attenuation, without regard to the variability among the months as a function of CD. At high values of CD, the adverse (maximum envelope) yearly tolerances can be as high as 40% of the year-average value of an effect. It should be noted that adverse tolerances for both noise temperature and attenuation give INCREASES from the values in Tables 1 through 18. An adverse VALUE is a mean PLUS the adverse tolerance. For mission planning purposes, with no need to create a model for a specific month, it may be sufficient to use the year-average value at a particular CD, and use the maximum/minimum envelope values to define very conservative adverse/favorable tolerances, with triangular distribution. For specific-month planning purposes, it may be sufficient to use the values given in Tables 1 through 18, with $\pm 5\%$ tolerances (triangular distribution) as stated above. A very conservative approach (acknowledging that any individual month in the future can be well outside the historical range of available data) would be to use the "maximum" envelope as the model for a possible "bad" month. Note also, that for particular months, characterized by "bad weather", year-to-year variation of noise temperature and attenuation statistics can be quite large.

2.2 *Rainfall Statistics*

To assist the user in determining which months may have large rainfall-related atmospheric noise temperature and attenuation increases, rainfall data are presented for the three DSN antenna locations. Months with large average rainfall amounts may not necessarily correspond to months with large noise temperature and attenuation values. Comparison with Tables 1 through 18 should be made.

Table 19 presents the monthly and year-average rainfall amounts for the three DSN antenna locations. The Goldstone data (1973–2000) were taken at the administration center, located near the middle of the Goldstone antenna complex. Some antennas may be located as much as 10 miles from this location. The Canberra data (1966–2002) were taken at the Tidbinbilla Nature Reserve, located about 3 miles southwest of the antenna site. The Madrid data (1961–1990) are the averages of the rainfall at two locations: Avila, about 20 miles northwest of the antenna site, and Madrid (Quatro Vientos) about 20 miles east of the antenna site. Although these averages may not exactly reflect the rainfall at the antenna site, the relative monthly amounts are undoubtedly correct.

2.3 *Wind Loading*

The effect of wind loading must be modeled probabilistically, since wind velocity varies randomly over time and space. Figure 10 shows the probability distribution of wind speed for Goldstone. Similar data for the Madrid and Canberra complexes will be supplied when available. The wind load on a particular antenna is dependent on the design of that antenna. Consequently, information about wind-load effect on antenna gain is listed in the appropriate antenna module.

Statistics show that Goldstone is the windiest of the three Deep Space Network antenna complexes. The DSS 14 70-m antenna is *stowed* (pointed vertically) when wind gusts exceed 55 mph (88 km/hr). The frequency of occurrence of this event can be deduced from a relationship between wind gusts and average wind speed. This relationship is found to be: maximum hourly wind speed = $0.62 \times$ strongest gust. Thus, for 55-mph (88 km/hr) gusts, the maximum hourly wind speed is found to be 34 mph (55 km/hr). From Figure 10, it is seen that this speed is exceeded approximately 2 % (175 hours) of the year and 4 % (29 hours) of the worst month. Actual practice has shown that no antenna has been stowed more than about 10 hours per year due to excessive wind-gust occurrences.

2.4 *Hot Body Noise*

2.4.1 *Solar Noise*

The increase in system noise when tracking near the Sun depends on the intensity of solar radiation at the received frequency and on the position of the Sun relative to the antenna gain pattern. The subreflector support structure (typically a quadripod, but a tripod at the DSS 13 BWG antenna) introduces nonuniformities in the sidelobe structure. Increases in noise temperature are typically greater in directions at right angles to the planes established by the subreflector support legs and the center of the reflector surface. Thus, a quadripod-type antenna will have four enhanced regions of noise temperature, and a tripod-type antenna will have six. With an azimuth-elevation (AZ-EL) or X-Y mounted antenna, the plane containing the Sun-Earth-probe (SEP) angle will rotate through the sidelobes during a tracking pass. This causes the solar noise to fluctuate during a track even if the SEP angle is constant.

A large number of measurements were made at Goldstone from 1987 to 1996 to determine the system noise temperature effects of tracking near the Sun (within about five deg from the center of the solar disk). These measurements were made at S-, X-, and Ka-bands on both 26- and 34-meter antennas.

Figure 11 shows the 10.7-cm (2800-MHz) solar radio flux during solar cycle 23 (1996-2007, the expected “maximum” should have occurred in late 2000 or early 2001). The flux is measured in solar flux units (SFU) where one SFU = 1×10^{-22} W/m²/Hz. Updated solar flux predictions can be found at the National Oceanic and Atmospheric Administration (NOAA) Space Environment Center web site <<http://www.sec.noaa.gov/weekly.html>> (Solar Cycle Progression and Prediction Plots). Solar flux predictions can be used to model S- and X-band

solar noise temperature contributions using the ratio of predicted solar flux to the solar flux that existed at the time the antenna noise temperatures were measured.

The general characteristic of the 11-year cycle of 2800-MHz solar flux is a rapid rise to a peak approximately 4–5 years after the minimum, followed by a 7–6 year gradual decrease. From cycle to cycle, the peak flux can vary by as much as a factor of two. The 10.7-cm flux is varied during solar cycle 23 from a minimum of about 70 SFU during 1996 to a maximum of about 190 ± 20 SFU during 2000–2001 and returning to an expected minimum of about 70 SFU during 2006.

Figure 12 shows X-band system noise temperature increases as measured at the Goldstone DSS 15 HEF antenna. These measurements show the increased effect for the Sun located (offset) at right angles to the quadripod legs. The quadripod legs are arranged in an “X” configuration, with 90-deg spacing. The measurements were made in November 1987 (near the beginning of the solar cycle) with a measured 2800-MHz flux value of 101 SFU and an 8800-MHz flux value of 259 SFU. The following expression may be used as an upper limit of X-band solar noise contribution at DSS 15 as shown in Figure 12.

$$T_{\text{sun}} = 800e^{-2.0\theta}, \text{ K} \quad (6)$$

where

$$\theta = \text{offset angle between center of beam and center of solar disk, deg}$$

Figure 13 shows S-band (2295 MHz) total system noise temperature measurements made on the Goldstone DSS 16, 26-m antenna on December 20, 1989. This antenna has no quadripod, and it can be assumed that the noise temperature values shown are independent of solar “clock angle” around the center of the antenna beam. The reported 2800-MHz solar flux at the time of the experiment was 194 SFU; at 8800 MHz it was 290 SFU. Note that compared to the November 1987 flux (Figure 12), the 2800-MHz flux has nearly doubled, but the 8800-MHz flux has only increased about 12 percent. The S-band solar contribution shown in Figure 13 can be modeled as

$$T_{\text{sun}} = 1400e^{-1.4\theta}, \text{ K} \quad (7)$$

where

$$\theta = \text{offset angle between center of beam and center of solar disk, deg}$$

Figures 14 and 15 are contour plots of the DSS 12, 34-m HA–DEC total system noise temperature versus declination and cross-declination antenna pointing offsets. DSS 12 has been decommissioned since the measurements were made, but the figures are included because they are representative of the effects of the quadripod on solar noise at other antennas. The quadripod legs are arranged in a “+” configuration with 90-deg spacing, hence the peaks at right angles to the legs.

Figure 14 is a contour plot of total S-band system noise temperature versus declination and cross-declination antenna pointing offsets at DSS 12. The contour interval is 50 K. These measurements were made on January 12, 1990. On this day the reported 2800-MHz solar flux was 173 SFU.

Figure 15 is a contour plot of total X-band system noise temperature versus declination and cross-declination antenna pointing offsets at DSS 12. The contour interval, measurement date, and flux values are identical with those in Figure 14. The reported 8800-MHz solar flux was 272 SFU.

Figures 16 and 17 show the X-band (8.4-GHz) and Ka-band (32-GHz) solar noise contributions at the DSS 13, 34-m research and development beam waveguide antenna as a function of offset angle from the center of the sun. These data were taken during mid-March, 1996, when the 10.7-cm solar flux was about 70 SFU (the minimum at the end of solar cycle 22 and at the beginning of solar cycle 23) and should be considered as representative of what is expected at the operational DSN beam waveguide antennas.

The following expressions give an approximate upper envelope for the noise contributions shown in Figures 16 and 17 as a function of offset angle

$$T_{\text{sun}} = \begin{cases} 1400e^{-5.1\theta}, & 0.35 < \theta \leq 0.75 \text{deg} \\ 86e^{-1.4\theta}, & \theta > 0.75 \text{deg} \end{cases}, \text{ at X-band} \quad (8)$$

$$T_{\text{sun}} = \begin{cases} 5000e^{-6.6\theta}, & 0.35 < \theta \leq 0.75 \text{deg} \\ 100e^{-1.4\theta}, & \theta > 0.75 \text{deg} \end{cases}, \text{ at Ka-band.} \quad (9)$$

At offset angles less than 0.35 deg (0.08 deg from the edge of the solar disk), solar noise contributions are likely to be in excess of 300 K at both frequencies. At offsets greater than 4.0 degrees, the solar contribution is negligible.

All noise contribution expressions given above should be compared with values shown in the corresponding figures to assess their validity. Note that these expressions should be considered valid only for the flux values given at the time of measurement. For predictive purposes, Figure 11 may be used to obtain future predicted 2800-MHz solar flux, and the noise contributions at S- and X-band can be modeled as described below.

During the 11-year solar cycle, the S-band flux varies by a factor of 3 (reference Figure 11) while the corresponding X-band flux varies by a factor of 2. For cycle 23, when the S-band range is expected to be from 70 SFU to as much as 210 SFU, the X-band range is predicted to be from about 200 SFU to about 400 SFU. The predicted X-band flux can be derived from the predicted S-band flux by the following expression.

$$\text{FLUX, X} = 200 + \frac{200(\text{FLUX, S} - 70)}{140} \quad (10)$$

For example, in January 2003 the mean S-band flux is predicted to be 125 SFU (from Figure 11). The mean predicted X-band flux would be 264 SFU.

The predicted solar noise contribution can be calculated based on measured noise contributions described above. For example, using the equation provided for Figure 12 (Equation 6) and the predicted X-band solar flux in January of 2002 (264 SFU), the predicted X-band solar noise contribution for a 2-degree offset angle using the 34-m HEF antenna would be

$$T_{\text{sun}} = \frac{264}{259} 800e^{-2.0 \times 2.0} = 14.6 \text{ K} \quad (11)$$

At Ka-band, the solar flux varies little over the solar cycle and the relationship between noise temperature increase and offset angle depicted in Figure 17 can be used at all times.

Figure 18 shows examples of measured S-band system noise temperature made with a 64-m antenna tracking Pioneer 8 (November 1968, near the solar maximum) and Helios (April 1975, near the solar minimum). For all practical purposes, these curves may be used to predict S-band performance for the DSN 70-m antennas. The “maximum” and “minimum” curves for each month show the solar “clock angle” effect due to sidelobes at right angles to the quadripod legs.

Figure 19 shows a theoretical curve of X-band 70-m antenna noise temperature as a function of SEP angle. This curve is generated based on an assumed X-band blackbody disk temperature of 23,000 K, representing an “average” value during the solar cycle. An expression giving quiet Sun brightness temperature, T_b (K), as a function of wavelength (mm) has been found to be

$$T_b = 5672\lambda^{0.24517}, \quad \text{K} \quad (12)$$

For S-band (2.3 GHz), $T_b = 18700$ K. For X-band (8.5 GHz) $T_b = 13600$ K. For Ka-band (32 GHz) $T_b = 9750$ K. The active Sun may be expected to have an X-band brightness temperature of as much as two to four times as high as the 13600 K calculated above.

2.4.2 *Lunar Noise*

For an antenna pointed near the Moon, a noise temperature determination similar to that made for the Sun should be carried out. The blackbody disk temperature of the Moon is about 240 K, and its apparent diameter is almost exactly that of the Sun's (approximately 0.5 deg). Figures 12 through 19 may be used for lunar calculations, with the noise temperature values scaled by 240/23000. Figures 13, 14, 15, and 18 include clear-sky system noise temperatures, which must be subtracted out before scaling in order to determine the lunar noise temperature increase. Nevertheless, at offset angles greater than 2 deg, the lunar noise contribution is negligible.

2.4.3 Planetary Noise

The increase in system noise temperature when tracking near a planet can be calculated by the formula

$$T_{pl} = \left(\frac{T_k G d^2}{16 R^2} \right) e^{-2.77 \left(\frac{\theta}{\theta_0} \right)^2}, \text{ K} \quad (13)$$

where

- T_k = blackbody disk temperature of the planet, K
- d = planet diameter, km
- R = distance to planet, km
- θ = angular distance from planet center to antenna beam center
- θ_0 = antenna half-power beamwidth (full beamwidth at half power)
- G = antenna gain, ratio $\left[10^{(G(\text{dBi})/10)} \right]$, including atmospheric attenuation.

Table 20 presents all the parameters needed for calculation of planetary noise contributions. Also given are the maximum values of expected X-band noise contributions for the mean minimum distance from Earth, with the antenna beam pointed at the center of the planet ($\theta=0$). Corresponding S-band noise temperature increases will be approximately 1/13 as large as the X-band increases because of the lower antenna gain (wider beamwidth) at the lower frequency.

In the case of Jupiter, there is a significant and variable non-thermal component of the noise temperature. Thus the effective blackbody disk temperature at S-band appears to be much higher than at X-band. The S-band noise temperature increase will be approximately 1/6 the X-band values for average Jupiter emission; it will be about 1/3 the X-band values for maximum Jupiter emission. Except for Venus and Jupiter at inferior conjunction (minimum distance), the noise contribution from the planets at S-band is negligible.

The expression for T_{pl} assumes that the angular extent of the radiating source is small compared to the antenna beamwidth. This approximation is adequate at X-band except for Venus near inferior conjunction (apparent diameter = 0.018 deg) using a 70-m antenna at X-band (beamwidth = 0.032 deg). At Ka-band with a 34-m antenna (beamwidth = 0.0174 deg), the approximation is not adequate for Venus near inferior conjunction and may not be adequate for Mars near inferior conjunction (apparent diameter = 0.005 deg). The expression also assumes that the antenna main beam has a Gaussian shape, with circular symmetry. Antenna gains and half-power beamwidths are given in modules 101, 102, 103, and 104.

2.4.4 *Galactic Noise*

The center of the Milky Way galaxy is located near -30 degrees declination, $17^{\text{h}}\,40^{\text{min}}$ right ascension. It is possible for a spacecraft with a declination of -30 deg to be in the vicinity of the galactic center, and an increase of system noise temperature would then be observed. A declination of -30 degrees is not typically achieved by spacecraft moving in the plane of the ecliptic, but there are some circumstances (for example, a flight out of the ecliptic) where this location may be observed. Galactic noise temperature contributions at frequencies above 10 GHz are typically insignificant. At S-band, looking directly at the galactic center, a noise temperature increase of about 10 K would be observed. A map of the galactic noise distribution can be seen in chapter 8 of the classic reference J. D. Kraus, *Radio Astronomy*, Cygnus-Quasar Books, Powell, Ohio, 1986.

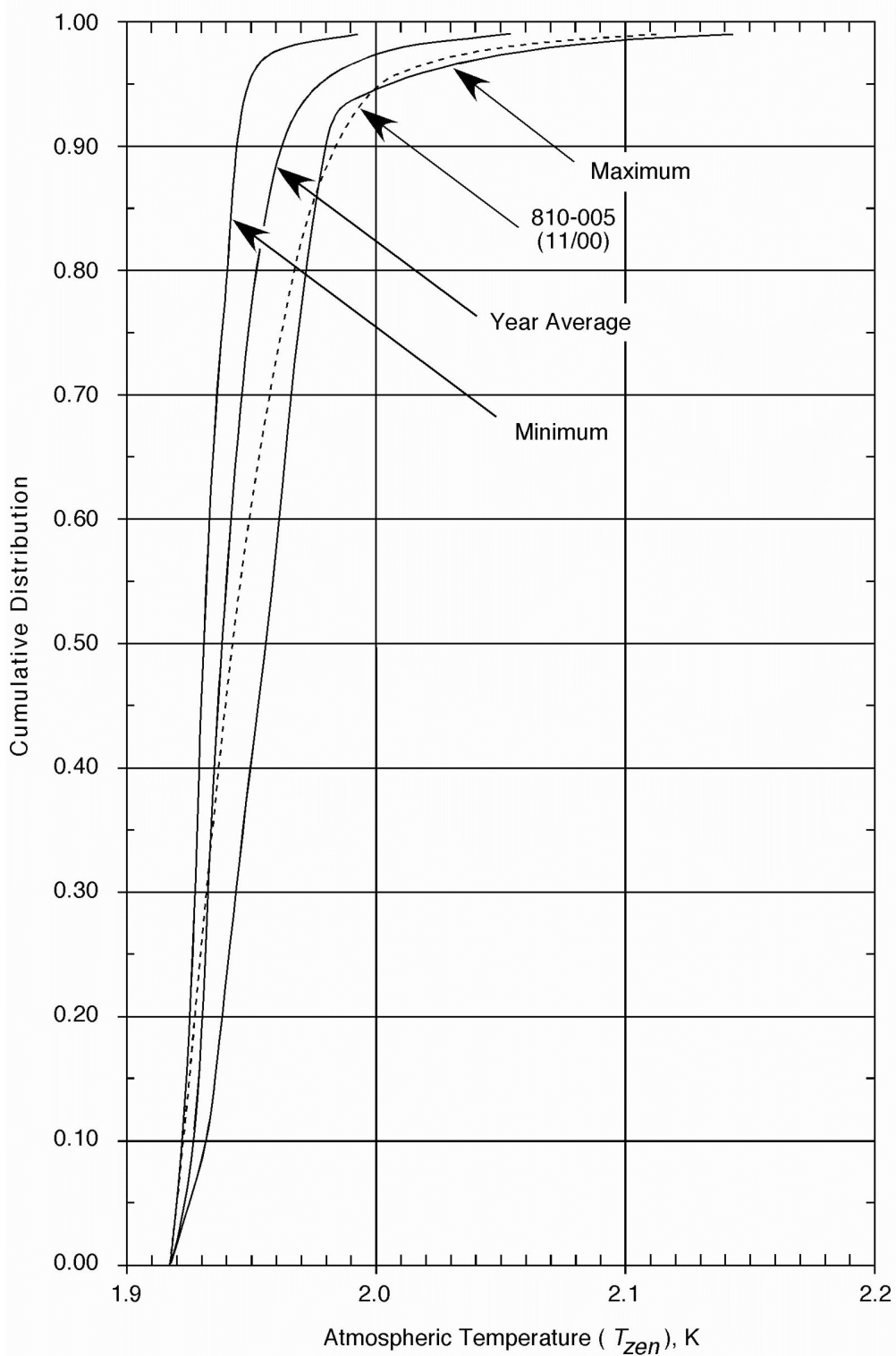


Figure 1. Cumulative Distributions of Zenith Atmospheric Noise Temperature at L-Band and S-Band, Goldstone DSCC

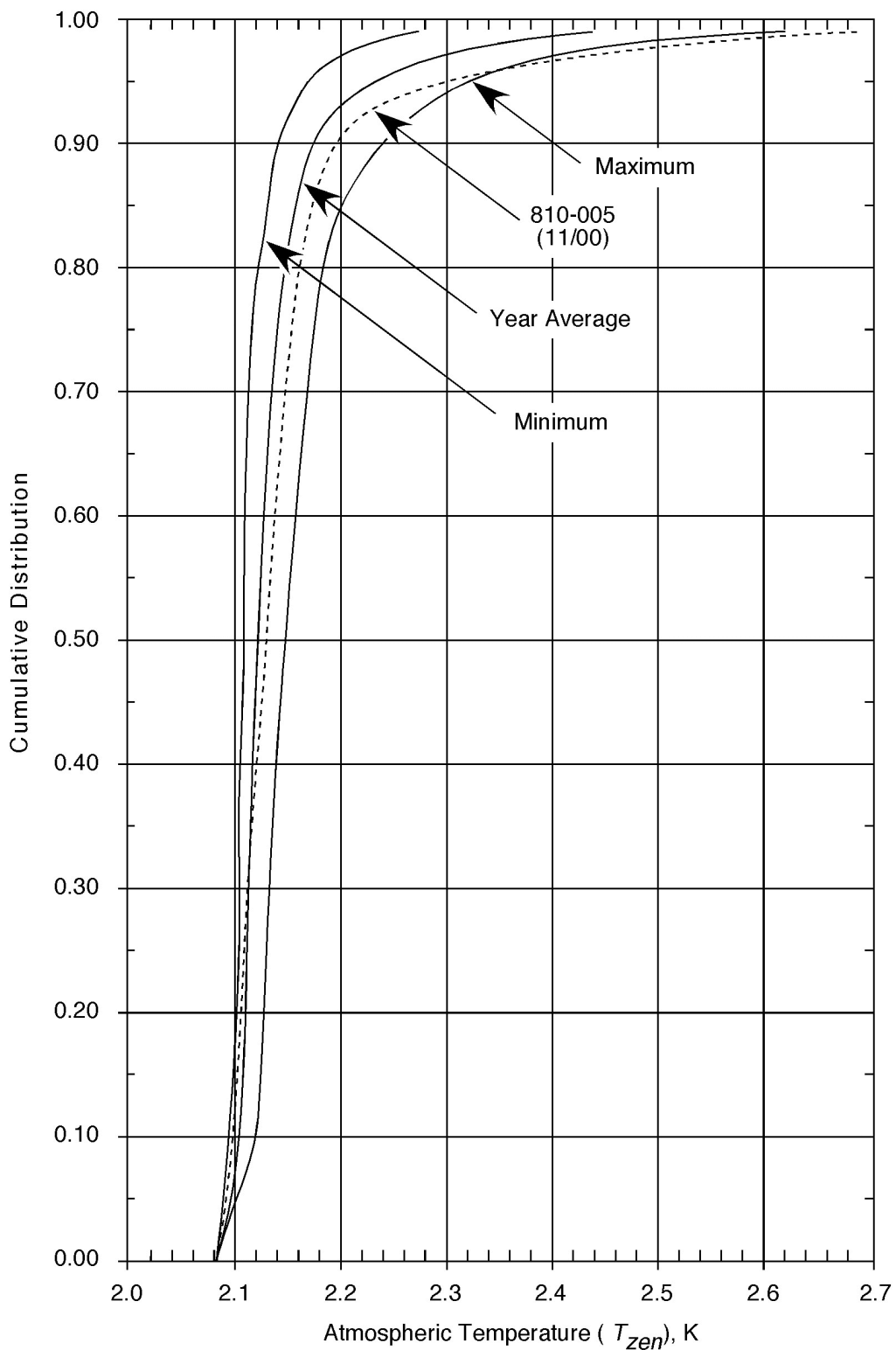


Figure 2. Cumulative Distributions of Zenith Atmospheric Noise Temperature at L-Band and S-Band, Canberra DSCC

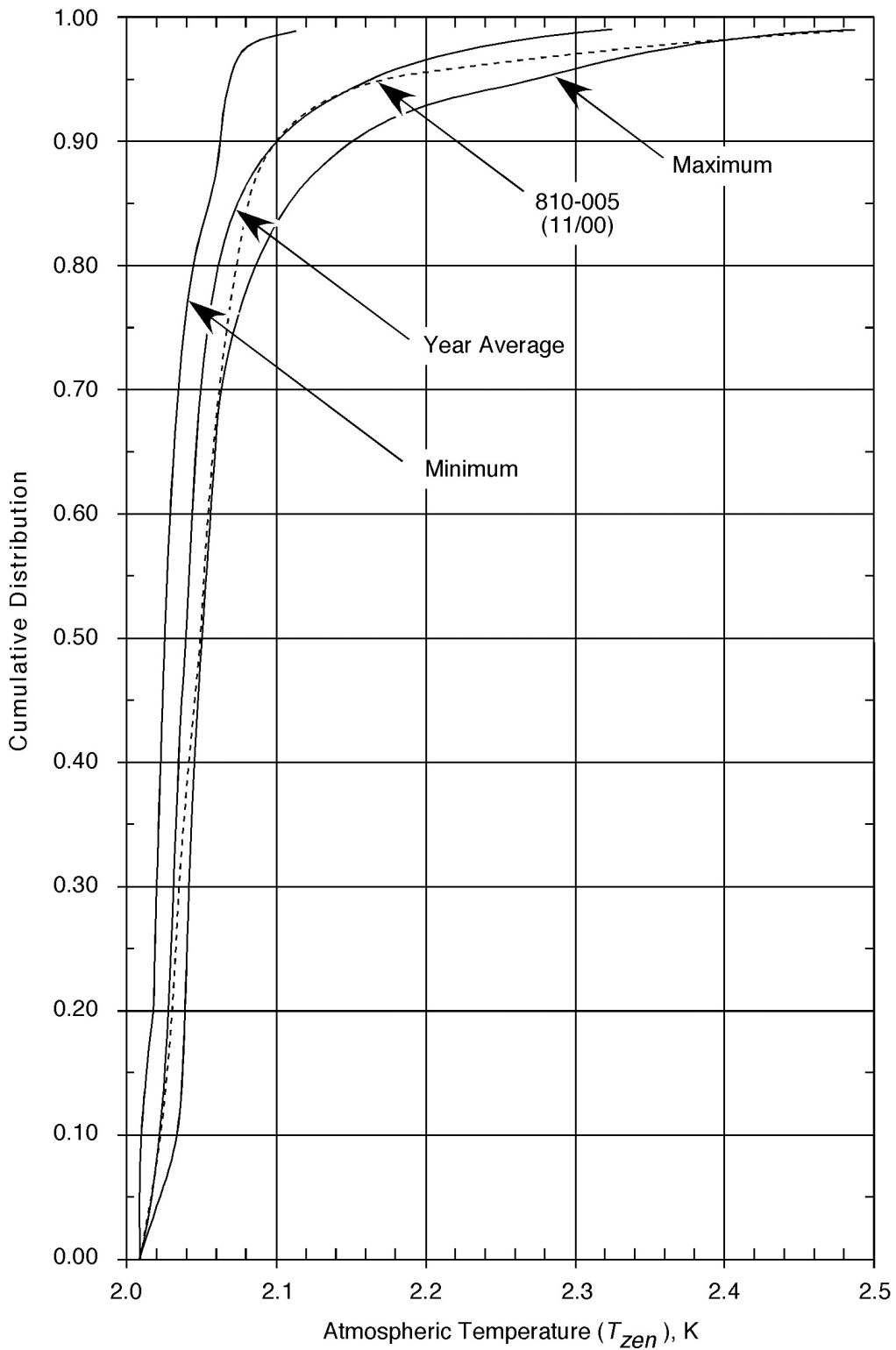


Figure 3. Cumulative Distributions of Zenith Atmospheric Noise Temperature at L-Band and S-Band, Madrid DSCC

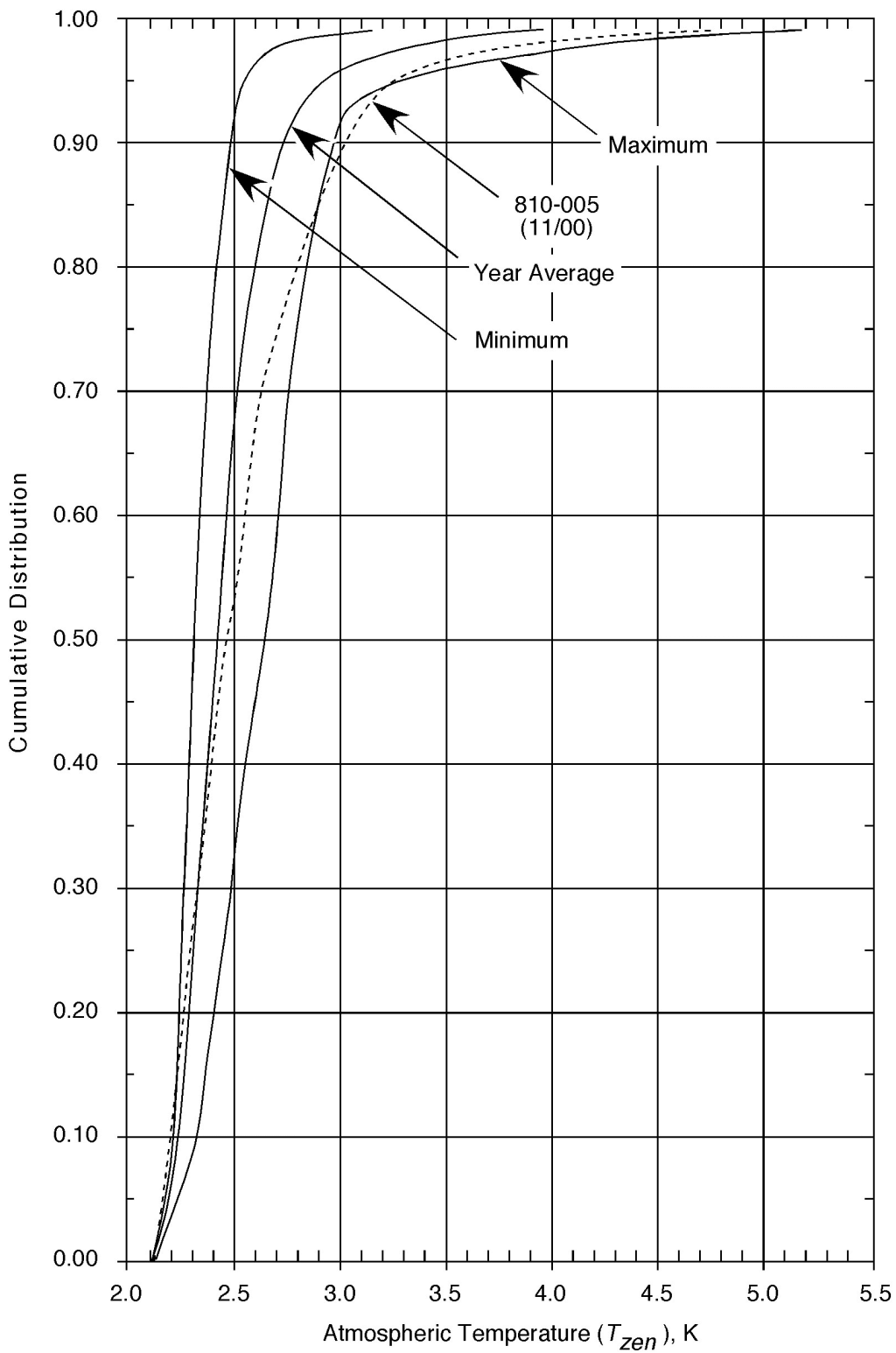


Figure 4. Cumulative Distributions of Zenith Atmospheric Noise Temperature at X-Band, Goldstone DSCC

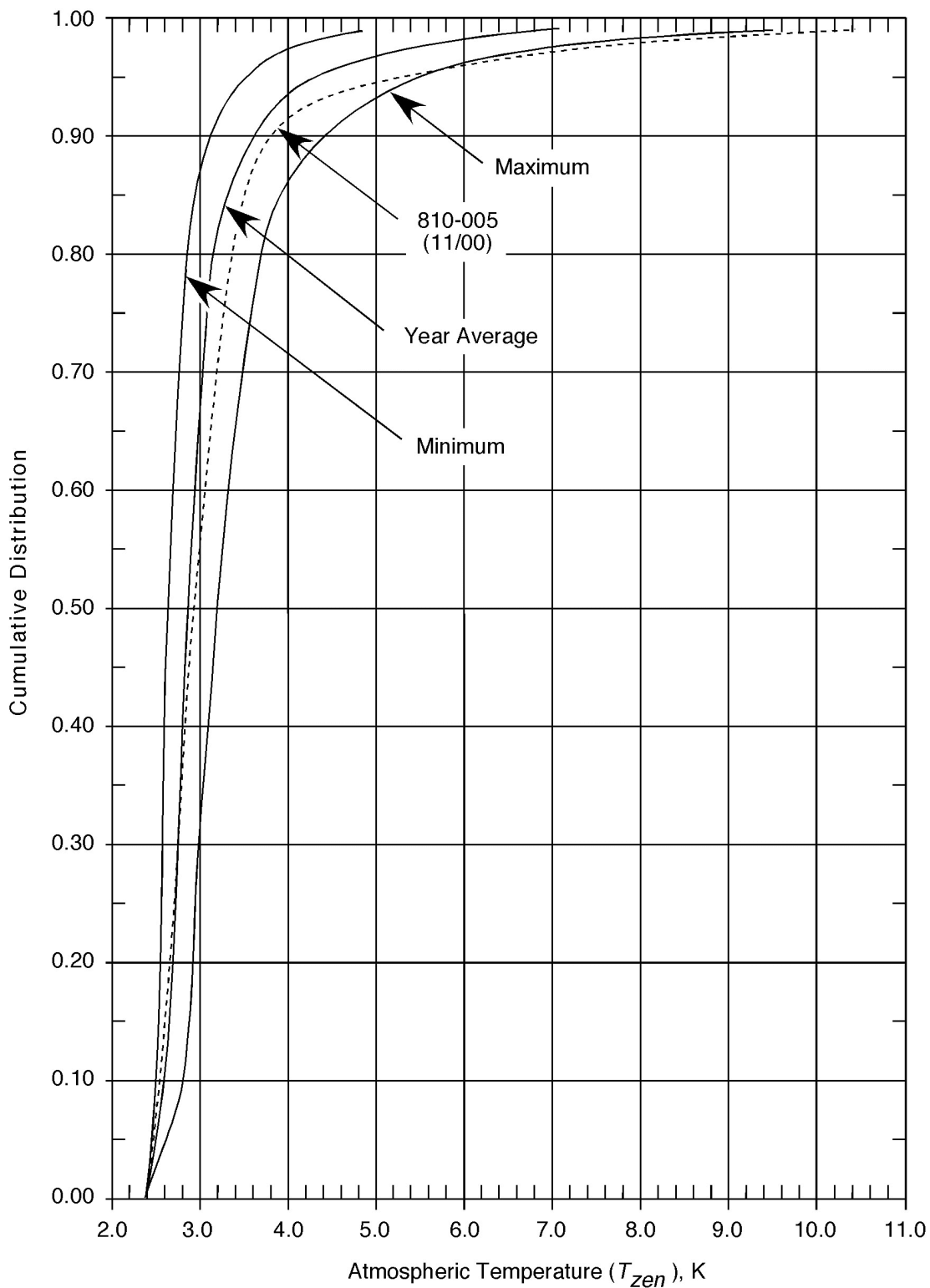


Figure 5. Cumulative Distributions of Zenith Atmospheric Noise Temperature at X-Band, Canberra DSCC

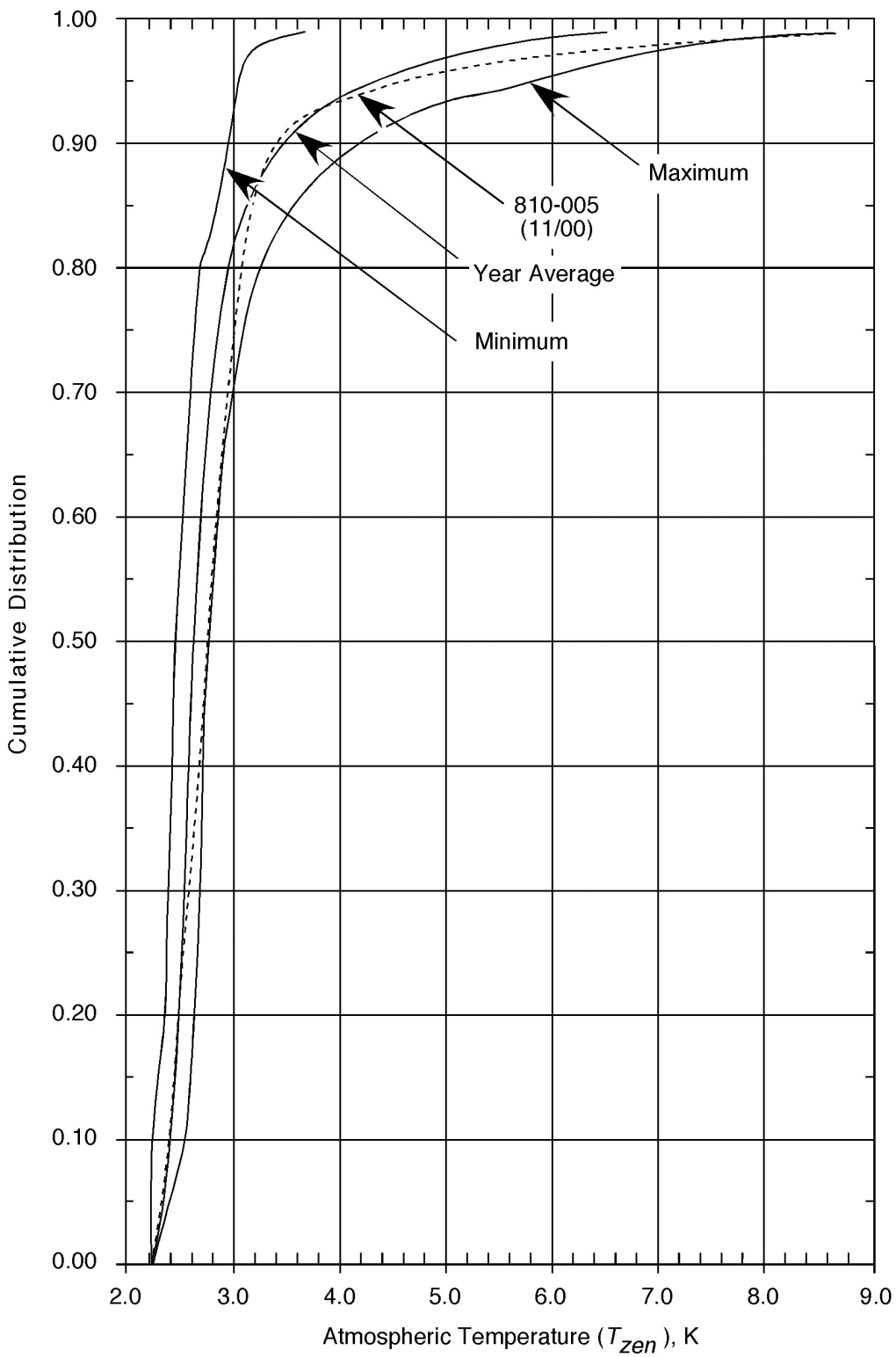


Figure 6. Cumulative Distributions of Zenith Atmospheric Noise Temperature at X-Band, Madrid DSCC

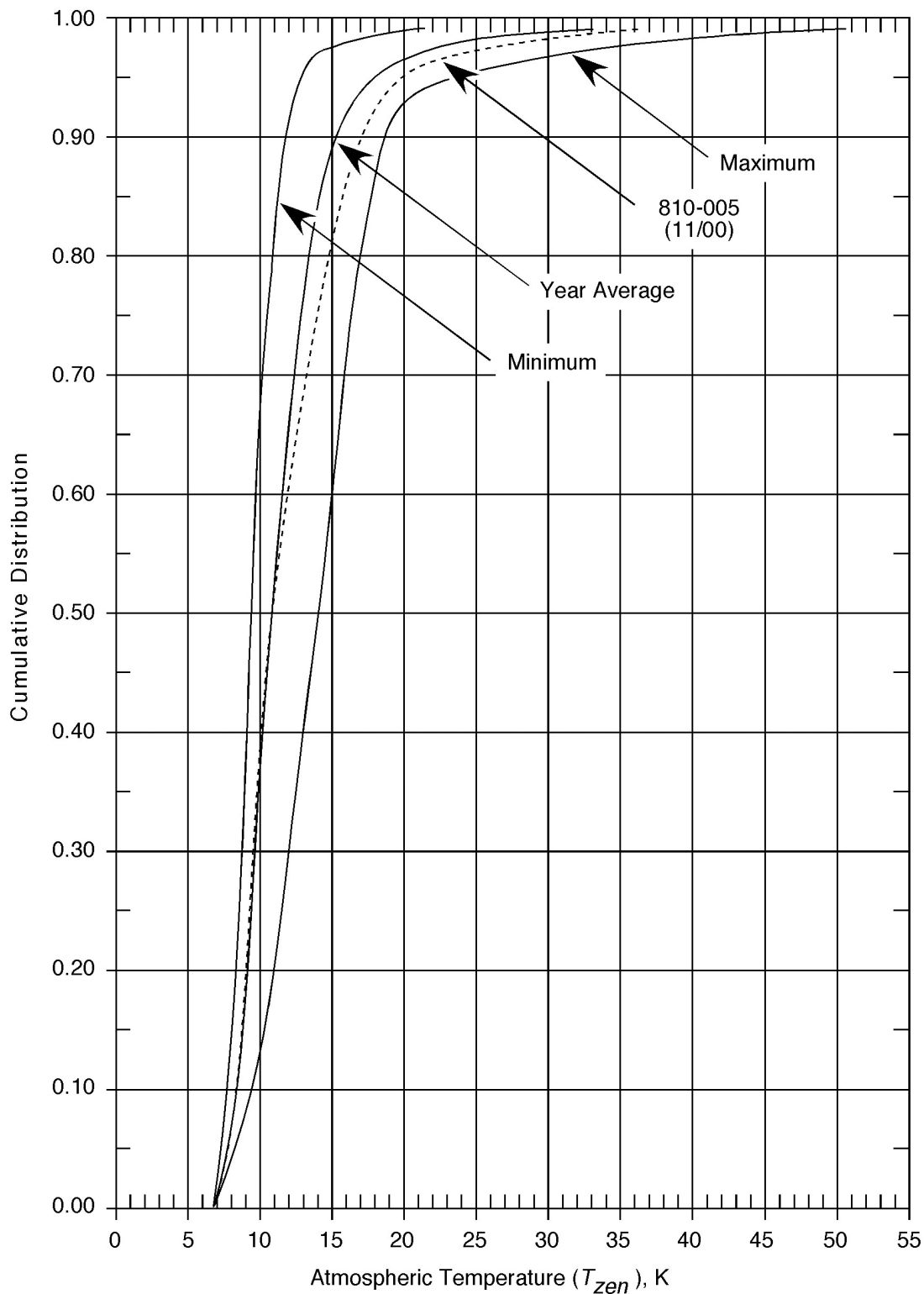


Figure 7. Cumulative Distributions of Zenith Atmospheric Noise Temperature at Ka-Band, Goldstone DSCL

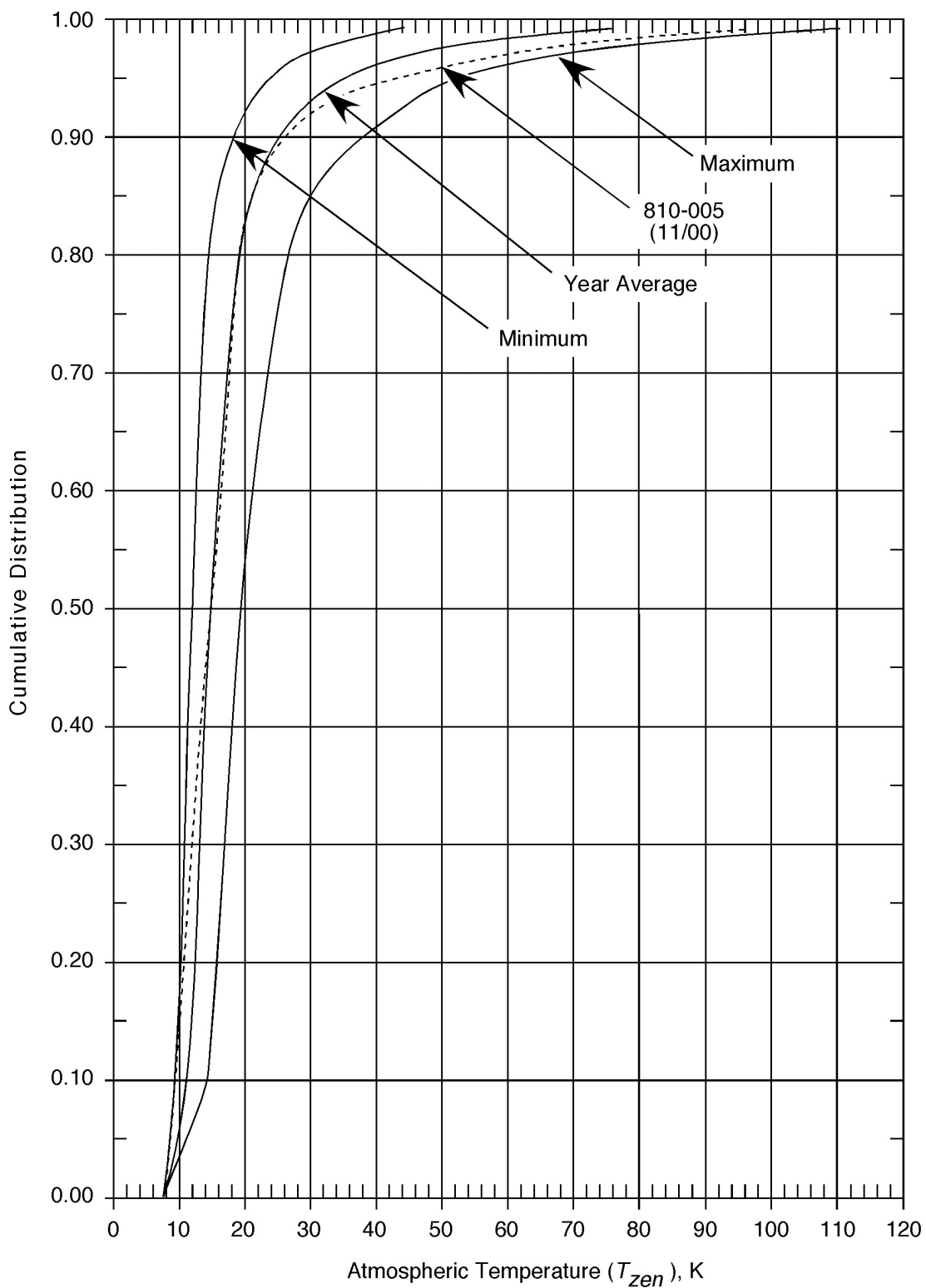


Figure 8. Cumulative Distributions of Zenith Atmospheric Noise Temperature at Ka-Band, Canberra DSCL

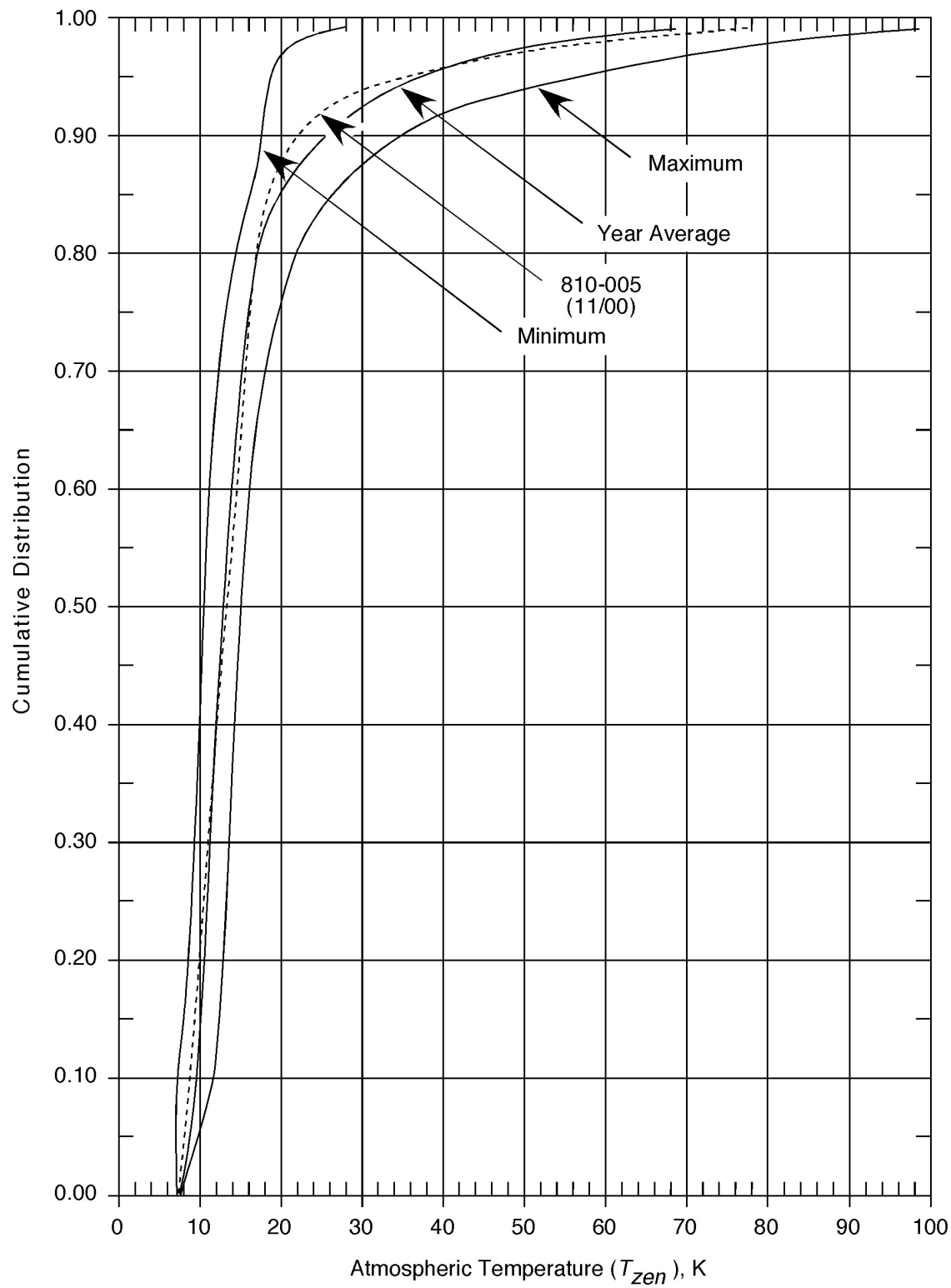


Figure 9. Cumulative Distributions of Zenith Atmospheric Noise Temperature at Ka-Band, Madrid DSCC

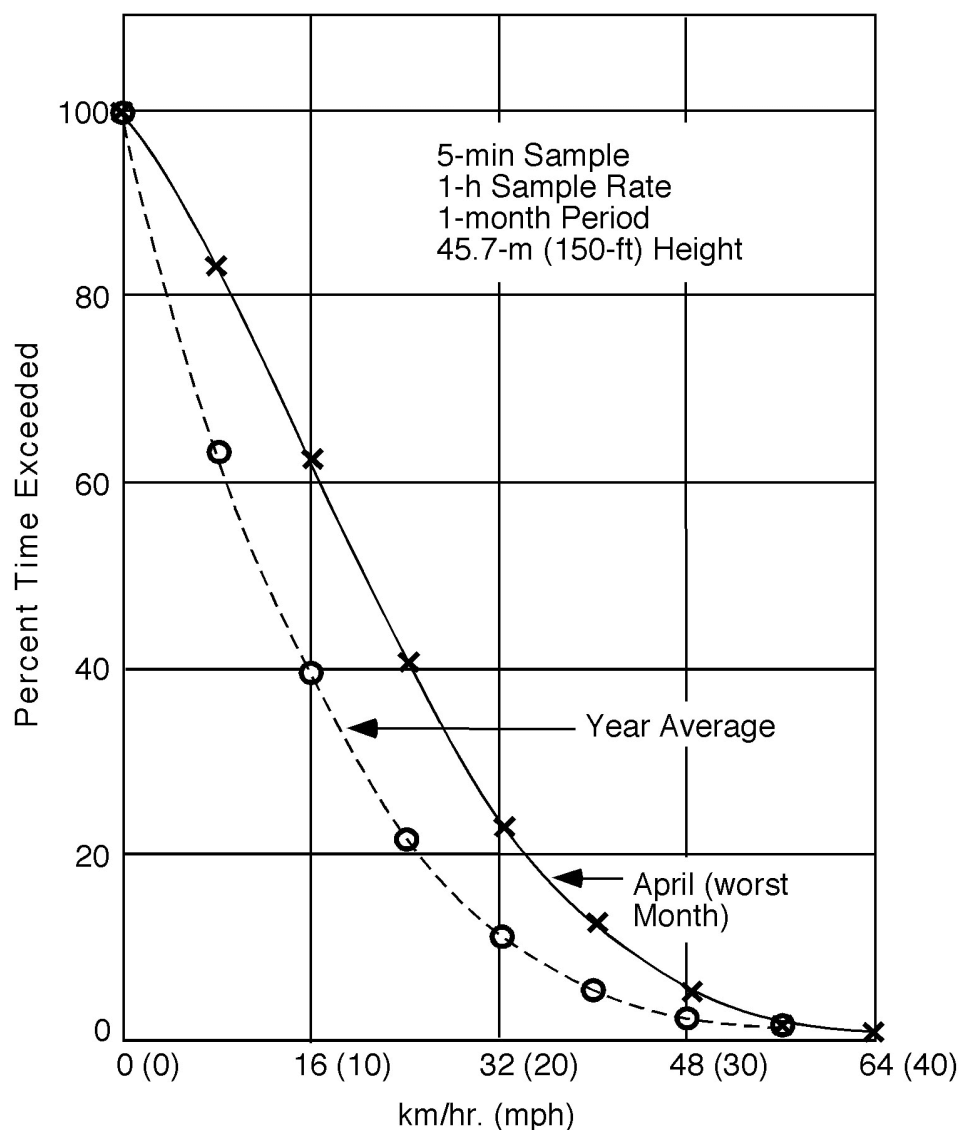


Figure 10. Probability Distribution of Wind Conditions at Goldstone

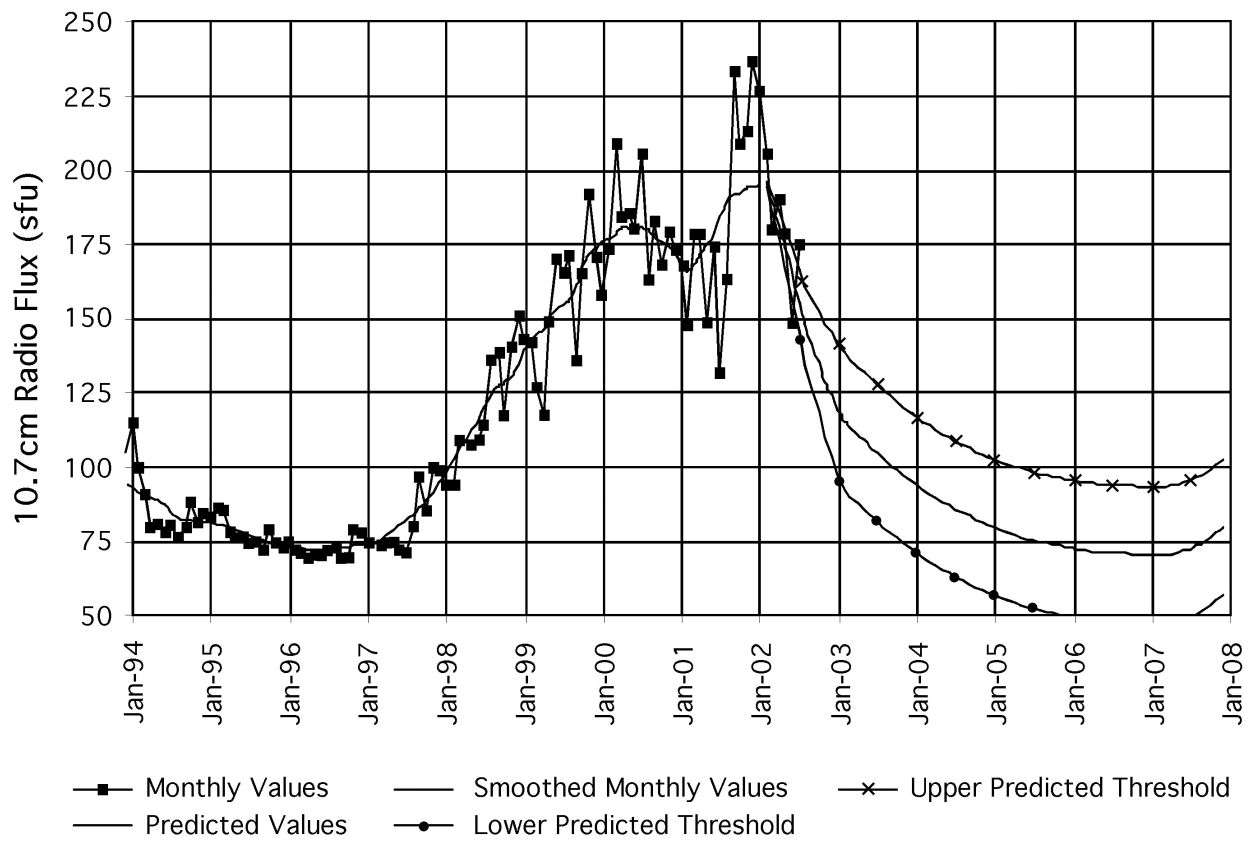


Figure 11. Solar Radio Flux at 2800 MHz (10.7 cm wavelength) During Solar Cycle 23 (1996–2007)

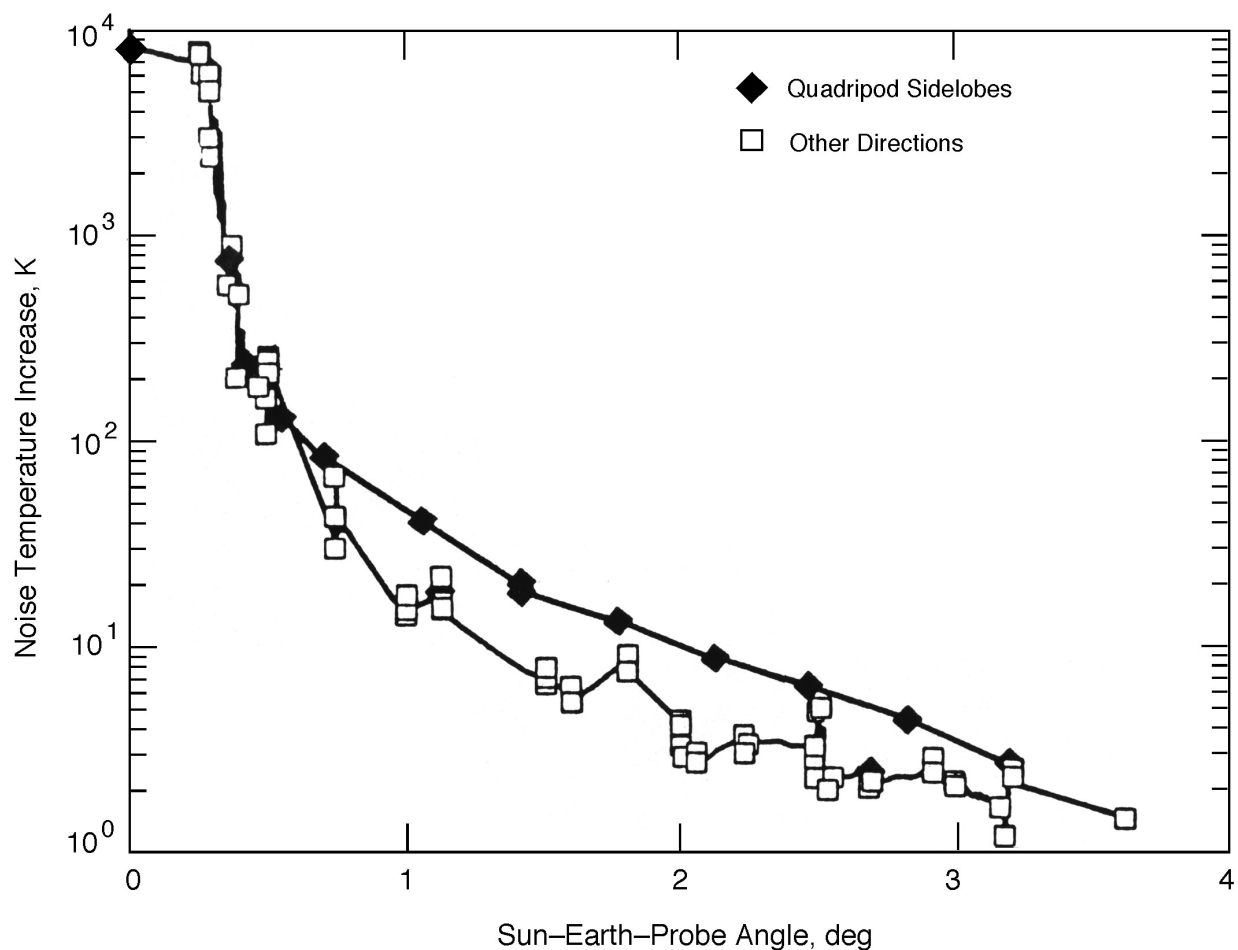


Figure 12. DSS 15 HEF Antenna X-Band System Noise Temperature Increases Due to the Sun at Various Offset Angles, Showing Larger Increases Perpendicular to Quadripod Directions

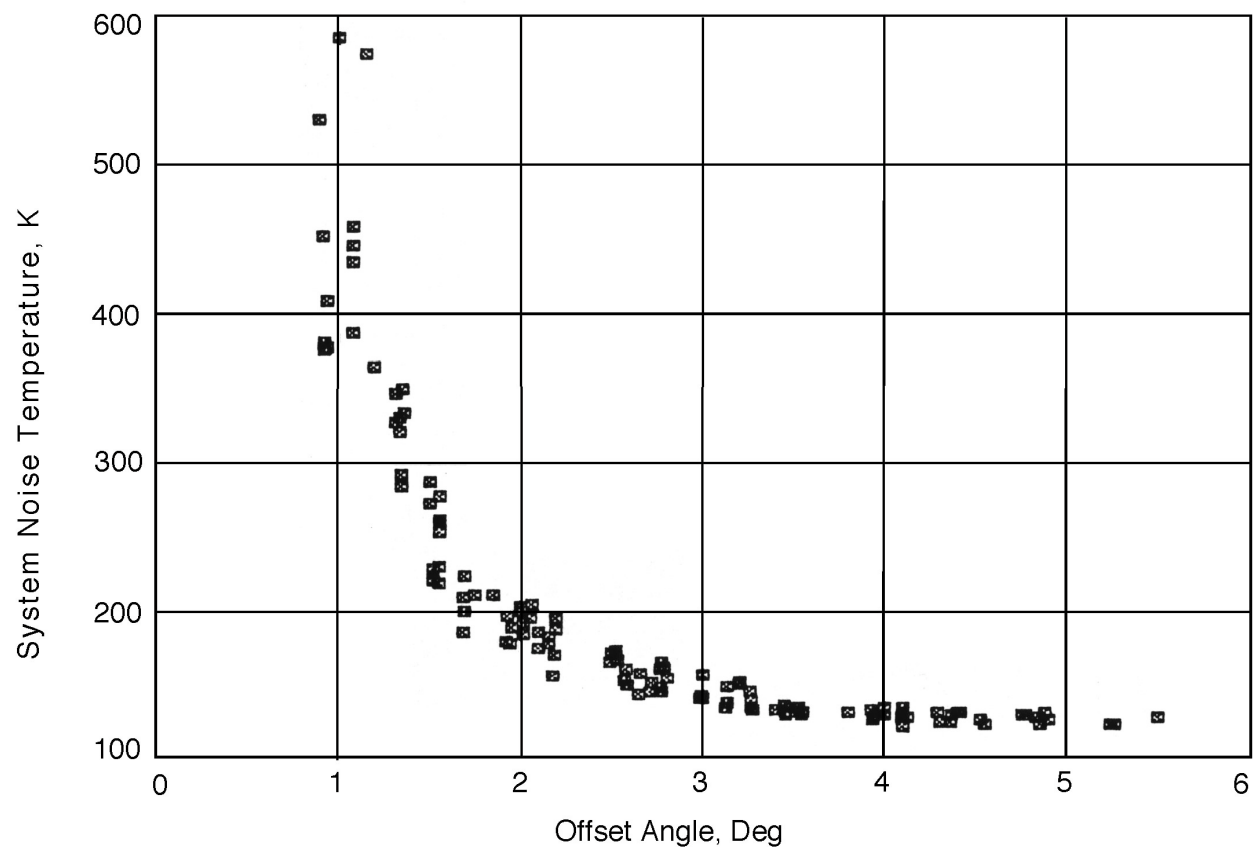


Figure 13. DSS 16 S-Band Total System Noise Temperature at Various Offset Angles from the Sun

810-005, Rev. E
105, Rev. A

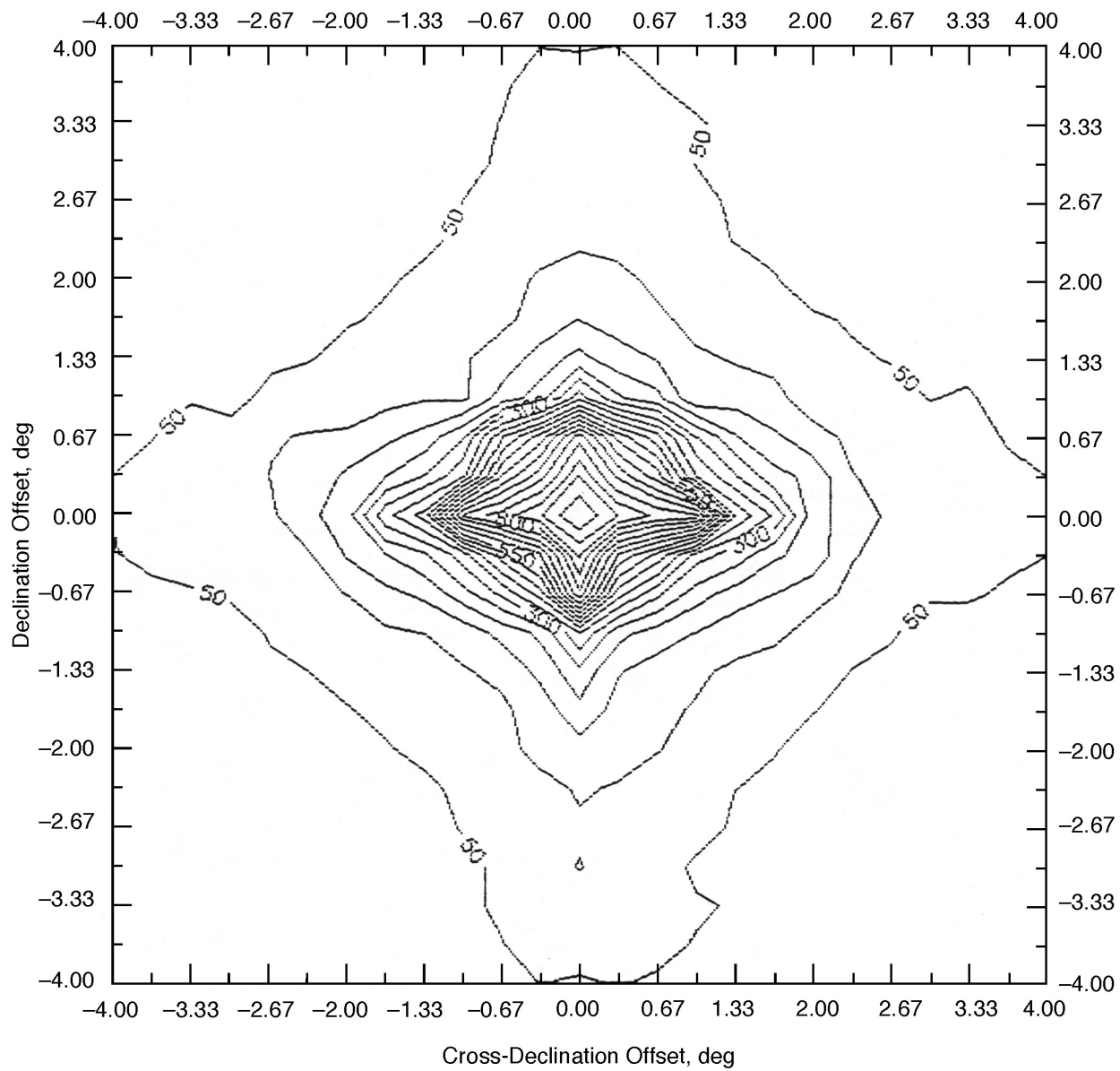


Figure 14. DSS 12 S-Band Total System Noise Temperature at Various Declination and Cross-Declination Offsets from the Sun

810-005, Rev. E
105, Rev. A

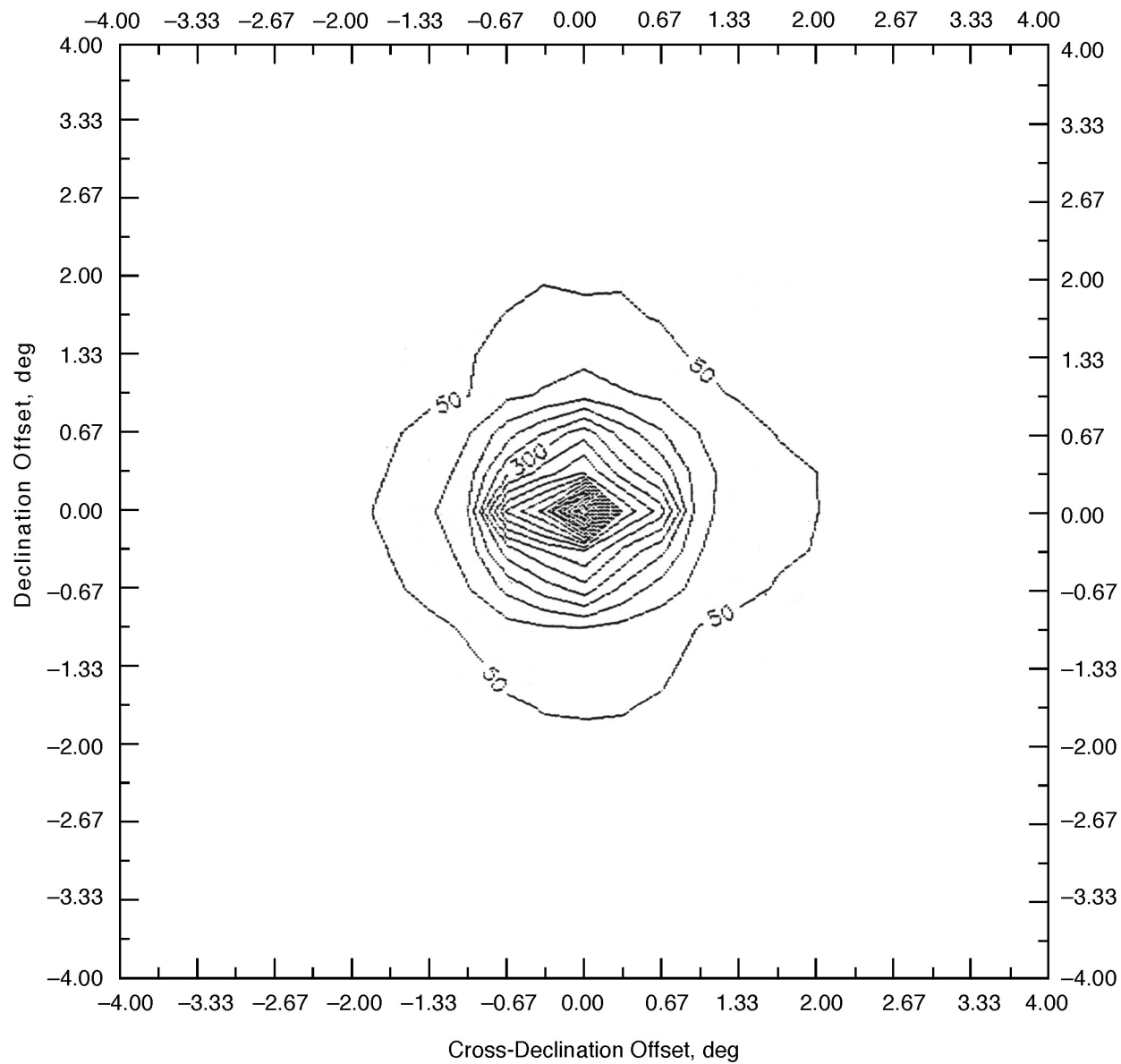


Figure 15. DSS 12 X-Band Total System Noise Temperature at Various Declination and Cross-Declination Offsets from the Sun

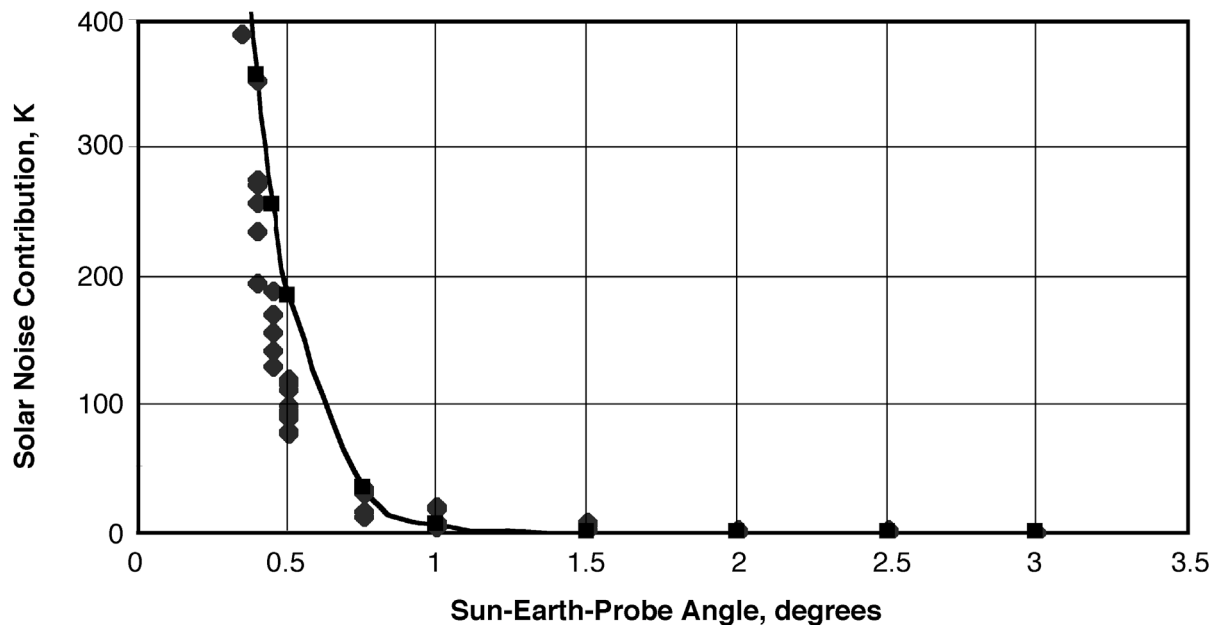


Figure 16. DSS 13 Beam-Waveguide Antenna X-Band Noise Temperature Increase Versus Offset Angle, March 1996

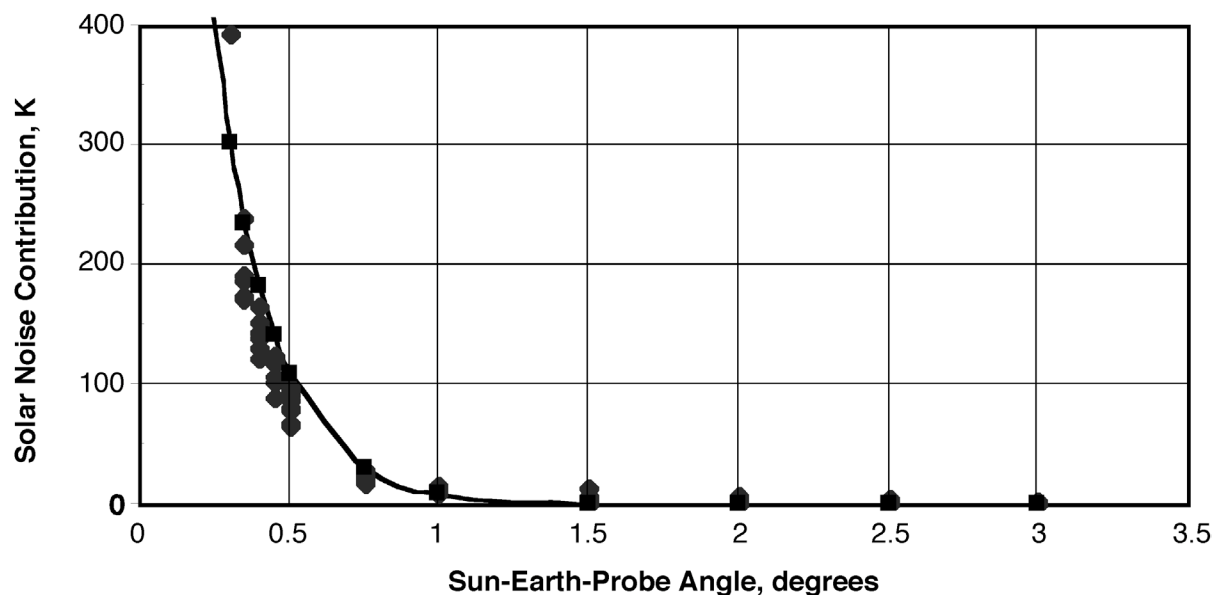


Figure 17. DSS 13 Beam-Waveguide Antenna Ka-Band Noise Temperature Increase Versus Offset Angle, March 1996

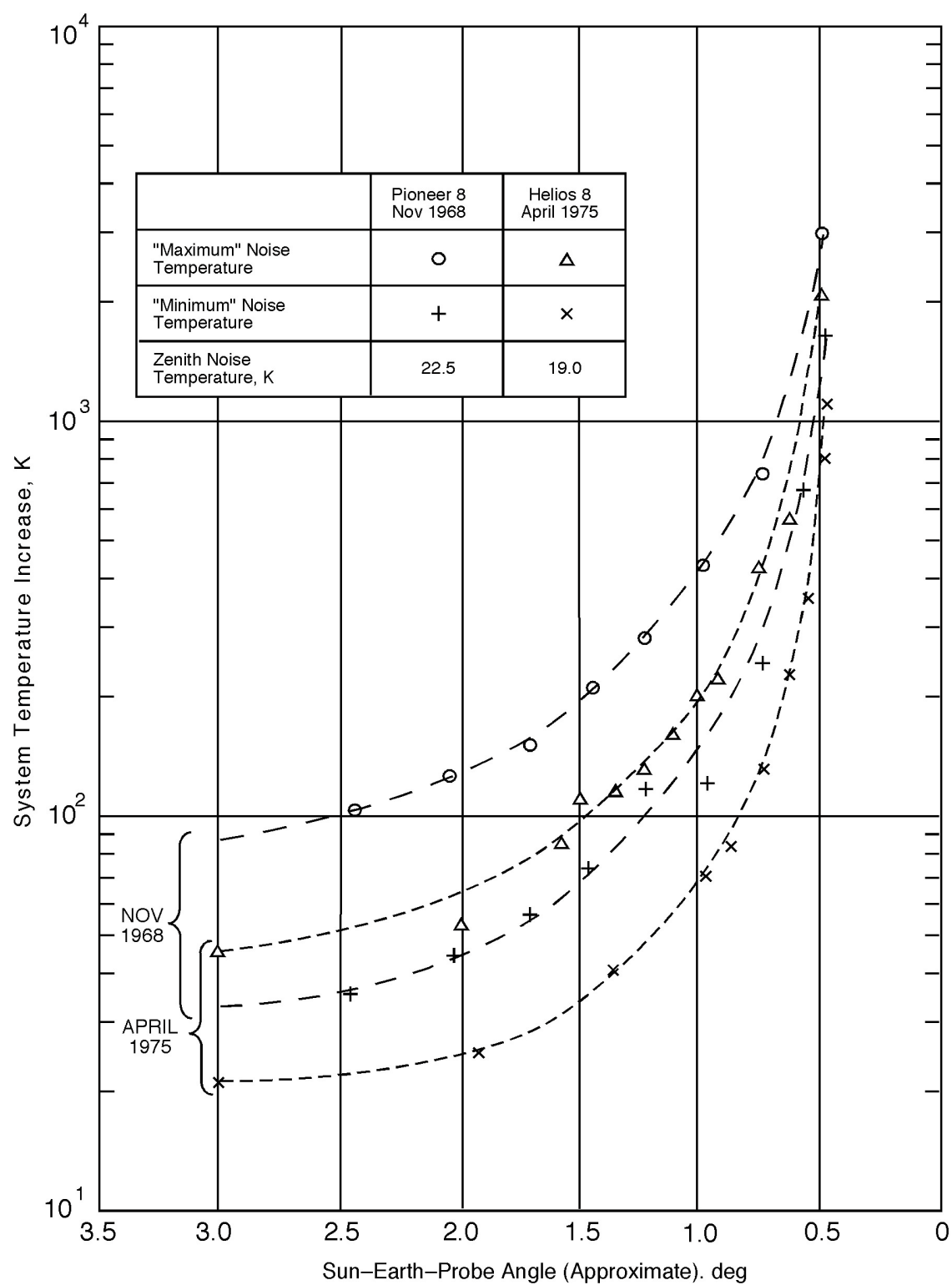


Figure 18. Total S-Band System Noise Temperature for 70-m Antennas Tracking Spacecraft Near the Sun (Derived from 64-m Measurements)

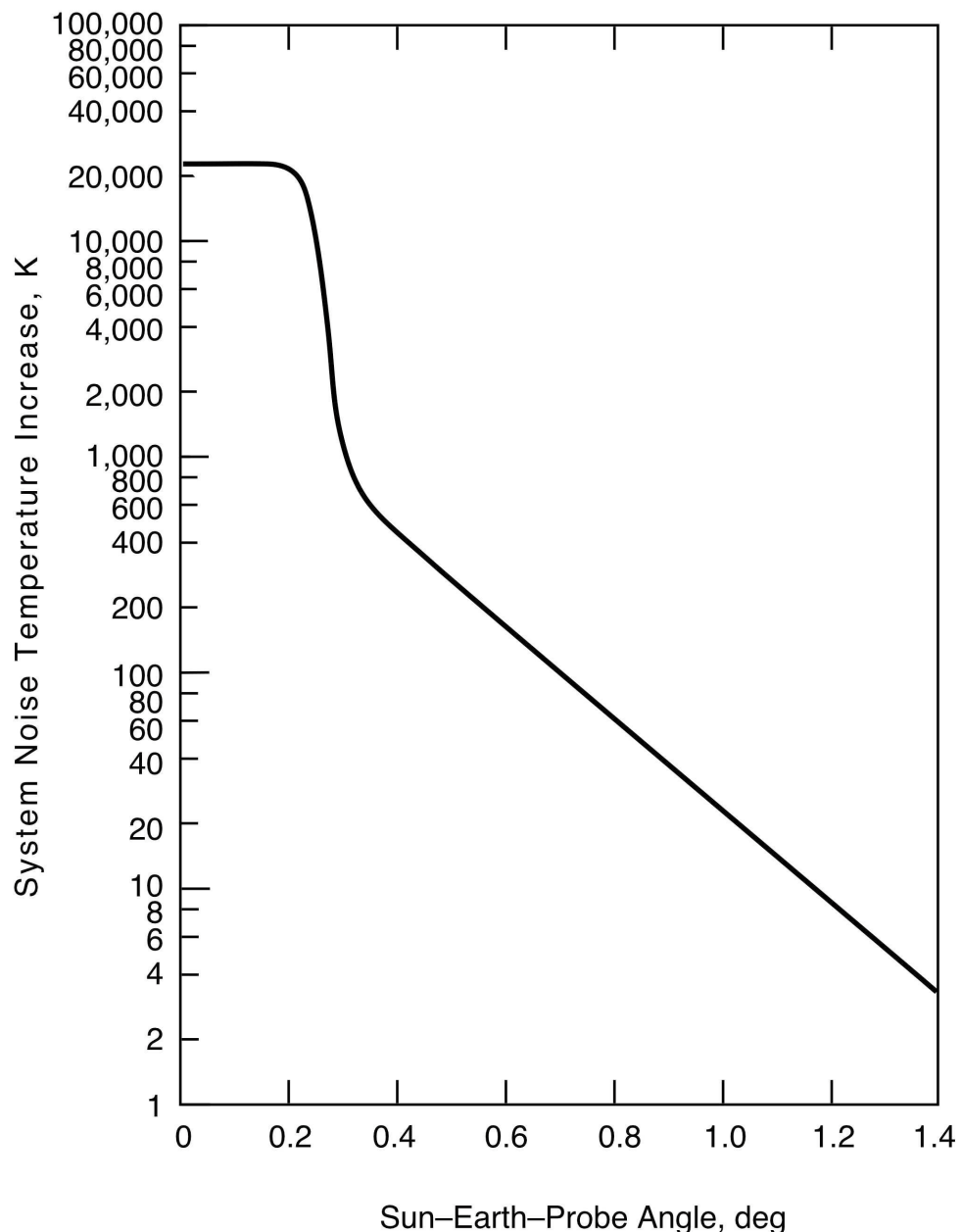


Figure 19. X-Band Noise Temperature Increase for 70-m Antennas as a Function of Sun-Earth-Probe Angle, Nominal Sun, 23,000 K Disk Temperature

Table 1. Cumulative Distributions of Zenith Atmospheric Noise Temperature at L- and S-Bands for Goldstone DSCL, K

CD	January	February	March	April	May	June
0.000	1.917	1.917	1.917	1.917	1.917	1.917
0.100	1.923	1.923	1.923	1.924	1.926	1.925
0.200	1.925	1.925	1.925	1.927	1.929	1.928
0.250	1.926	1.925	1.926	1.927	1.930	1.929
0.300	1.927	1.927	1.927	1.929	1.932	1.930
0.400	1.928	1.928	1.929	1.930	1.935	1.933
0.500	1.930	1.930	1.931	1.932	1.938	1.936
0.600	1.933	1.932	1.932	1.934	1.941	1.941
0.700	1.938	1.935	1.935	1.936	1.945	1.947
0.800	1.945	1.940	1.938	1.939	1.950	1.952
0.850	1.951	1.945	1.941	1.940	1.954	1.955
0.900	1.963	1.954	1.945	1.943	1.961	1.961
0.925	1.978	1.961	1.947	1.945	1.967	1.967
0.930	1.981	1.963	1.948	1.945	1.968	1.968
0.950	2.002	1.975	1.952	1.948	1.983	1.975
0.960	2.017	1.984	1.957	1.950	1.990	1.981
0.975	2.059	2.005	1.973	1.956	2.010	2.001
0.980	2.075	2.015	1.982	1.963	2.016	2.011
0.990	2.142	2.051	2.022	1.992	2.042	2.051

Table 1 (Cont'd). Cumulative Distributions of Zenith Atmospheric Noise Temperature at L- and S-Bands for Goldstone DSCL, K

CD	July	August	September	October	November	December	Minimum	Year Average	Maximum
0.000	1.917	1.917	1.917	1.917	1.917	1.917	1.917	1.917	1.917
0.100	1.929	1.930	1.932	1.927	1.924	1.922	1.922	1.926	1.932
0.200	1.934	1.935	1.935	1.930	1.926	1.925	1.925	1.929	1.935
0.250	1.936	1.937	1.936	1.930	1.927	1.925	1.925	1.930	1.937
0.300	1.938	1.940	1.939	1.932	1.929	1.927	1.927	1.931	1.940
0.400	1.942	1.945	1.943	1.935	1.931	1.928	1.928	1.934	1.945
0.500	1.947	1.951	1.948	1.937	1.934	1.930	1.930	1.937	1.951
0.600	1.954	1.955	1.952	1.940	1.939	1.932	1.932	1.941	1.955
0.700	1.962	1.959	1.958	1.943	1.943	1.935	1.935	1.945	1.962
0.800	1.969	1.963	1.964	1.948	1.948	1.941	1.938	1.950	1.969
0.850	1.972	1.967	1.967	1.952	1.952	1.947	1.940	1.954	1.972
0.900	1.977	1.972	1.975	1.958	1.958	1.957	1.943	1.960	1.977
0.925	1.981	1.976	1.980	1.961	1.961	1.964	1.945	1.966	1.981
0.930	1.982	1.976	1.980	1.961	1.961	1.967	1.945	1.967	1.982
0.950	1.987	1.983	1.986	1.966	1.965	1.985	1.948	1.975	2.002
0.960	1.991	1.987	1.992	1.970	1.968	1.997	1.950	1.982	2.017
0.975	2.003	2.000	2.008	1.983	1.978	2.028	1.956	2.000	2.059
0.980	2.011	2.001	2.024	1.990	1.989	2.042	1.963	2.010	2.075
0.990	2.049	2.009	2.098	2.025	2.031	2.098	1.992	2.051	2.142

Table 2. Cumulative Distributions of Zenith Atmospheric Noise Temperature at L- and S-Bands for Canberra DSCC, K

CD	January	February	March	April	May	June
0.000	2.085	2.085	2.085	2.085	2.085	2.085
0.100	2.108	2.116	2.121	2.106	2.100	2.099
0.200	2.115	2.123	2.127	2.111	2.103	2.105
0.250	2.117	2.127	2.129	2.113	2.104	2.106
0.300	2.120	2.131	2.131	2.115	2.106	2.107
0.400	2.124	2.139	2.137	2.119	2.108	2.109
0.500	2.132	2.147	2.141	2.123	2.111	2.112
0.600	2.139	2.156	2.149	2.128	2.114	2.115
0.700	2.148	2.168	2.158	2.133	2.119	2.118
0.800	2.159	2.183	2.167	2.143	2.133	2.124
0.850	2.166	2.198	2.174	2.150	2.143	2.129
0.900	2.180	2.239	2.187	2.164	2.164	2.140
0.925	2.193	2.271	2.202	2.186	2.190	2.157
0.930	2.196	2.278	2.207	2.191	2.198	2.165
0.950	2.220	2.319	2.231	2.217	2.239	2.204
0.960	2.236	2.346	2.244	2.236	2.269	2.221
0.975	2.286	2.428	2.281	2.288	2.339	2.261
0.980	2.316	2.475	2.310	2.314	2.358	2.281
0.990	2.476	2.616	2.394	2.387	2.439	2.330

Table 2 (Cont'd). Cumulative Distributions of Zenith Atmospheric Noise Temperature at L- and S-Bands for Canberra DSCC, K

CD	July	August	September	October	November	December	Minimum	Year Average	Maximum
0.000	2.085	2.085	2.085	2.085	2.085	2.085	2.085	2.085	2.085
0.100	2.097	2.097	2.101	2.102	2.109	2.102	2.097	2.105	2.121
0.200	2.100	2.101	2.105	2.107	2.114	2.109	2.100	2.110	2.127
0.250	2.102	2.102	2.107	2.108	2.117	2.112	2.102	2.112	2.129
0.300	2.103	2.103	2.108	2.110	2.119	2.115	2.103	2.114	2.131
0.400	2.105	2.105	2.112	2.113	2.124	2.120	2.105	2.118	2.139
0.500	2.108	2.107	2.115	2.117	2.129	2.125	2.107	2.122	2.147
0.600	2.111	2.110	2.119	2.123	2.135	2.132	2.110	2.128	2.156
0.700	2.115	2.114	2.125	2.131	2.144	2.141	2.114	2.134	2.168
0.800	2.122	2.121	2.133	2.146	2.162	2.157	2.121	2.146	2.183
0.850	2.128	2.128	2.140	2.158	2.179	2.172	2.128	2.155	2.198
0.900	2.138	2.144	2.152	2.181	2.206	2.197	2.138	2.174	2.239
0.925	2.151	2.161	2.164	2.208	2.232	2.219	2.151	2.195	2.271
0.930	2.155	2.166	2.169	2.215	2.239	2.227	2.155	2.200	2.278
0.950	2.171	2.190	2.198	2.262	2.279	2.261	2.171	2.233	2.319
0.960	2.183	2.212	2.220	2.288	2.303	2.278	2.183	2.253	2.346
0.975	2.209	2.285	2.266	2.365	2.392	2.322	2.209	2.310	2.428
0.980	2.223	2.309	2.296	2.414	2.432	2.343	2.223	2.339	2.475
0.990	2.274	2.394	2.423	2.532	2.547	2.412	2.274	2.435	2.616

Table 3. Cumulative Distributions of Zenith Atmospheric Noise Temperature at L- and S-Bands for Madrid DSAC, K

CD	January	February	March	April	May	June
0.000	2.008	2.008	2.008	2.008	2.008	2.008
0.100	2.014	2.013	2.018	2.019	2.026	2.029
0.200	2.017	2.017	2.022	2.023	2.031	2.034
0.250	2.018	2.018	2.023	2.024	2.032	2.035
0.300	2.020	2.019	2.025	2.026	2.034	2.037
0.400	2.023	2.022	2.028	2.028	2.038	2.041
0.500	2.027	2.025	2.031	2.032	2.041	2.044
0.600	2.032	2.029	2.035	2.036	2.044	2.047
0.700	2.042	2.034	2.041	2.042	2.048	2.051
0.800	2.066	2.042	2.052	2.054	2.057	2.055
0.850	2.092	2.054	2.063	2.066	2.075	2.059
0.900	2.139	2.077	2.088	2.084	2.114	2.065
0.925	2.192	2.102	2.116	2.102	2.155	2.070
0.930	2.201	2.107	2.122	2.106	2.163	2.072
0.950	2.272	2.145	2.157	2.142	2.211	2.085
0.960	2.299	2.167	2.179	2.163	2.237	2.098
0.975	2.361	2.227	2.237	2.211	2.298	2.140
0.980	2.380	2.247	2.259	2.225	2.320	2.169
0.990	2.450	2.324	2.335	2.276	2.394	2.282

Table 3 (Cont'd). Cumulative Distributions of Zenith Atmospheric Noise Temperature at L- and S-Bands for Madrid DSAC, K

CD	July	August	September	October	November	December	Minimum	Year Average	Maximum
0.000	2.008	2.008	2.008	2.008	2.008	2.008	2.008	2.008	2.008
0.100	2.032	2.032	2.029	2.023	2.008	2.013	2.008	2.021	2.032
0.200	2.036	2.037	2.034	2.031	2.018	2.018	2.017	2.026	2.037
0.250	2.037	2.038	2.036	2.033	2.020	2.020	2.018	2.028	2.038
0.300	2.039	2.040	2.038	2.036	2.023	2.023	2.019	2.030	2.040
0.400	2.043	2.043	2.042	2.041	2.026	2.027	2.022	2.033	2.043
0.500	2.045	2.047	2.046	2.047	2.030	2.032	2.025	2.037	2.047
0.600	2.048	2.050	2.051	2.054	2.036	2.038	2.029	2.042	2.054
0.700	2.052	2.053	2.055	2.062	2.044	2.049	2.034	2.048	2.062
0.800	2.055	2.058	2.061	2.082	2.058	2.073	2.042	2.059	2.082
0.850	2.057	2.060	2.065	2.105	2.079	2.099	2.054	2.073	2.105
0.900	2.061	2.064	2.072	2.147	2.121	2.142	2.061	2.098	2.147
0.925	2.063	2.067	2.079	2.189	2.164	2.181	2.063	2.123	2.192
0.930	2.064	2.067	2.081	2.197	2.171	2.187	2.064	2.128	2.201
0.950	2.067	2.071	2.095	2.256	2.229	2.235	2.067	2.164	2.272
0.960	2.069	2.074	2.110	2.283	2.253	2.257	2.069	2.182	2.299
0.975	2.077	2.083	2.159	2.350	2.316	2.316	2.077	2.231	2.361
0.980	2.084	2.090	2.196	2.377	2.333	2.334	2.084	2.251	2.380
0.990	2.117	2.119	2.333	2.481	2.400	2.397	2.117	2.326	2.481

Table 4. Cumulative Distributions of Zenith Atmospheric Noise Temperature at X-Band for Goldstone DSCC, K

CD	January	February	March	April	May	June
0.000	2.135	2.135	2.135	2.135	2.135	2.135
0.100	2.218	2.210	2.220	2.233	2.257	2.246
0.200	2.241	2.238	2.247	2.266	2.297	2.284
0.250	2.249	2.249	2.256	2.276	2.310	2.296
0.300	2.264	2.264	2.268	2.291	2.331	2.315
0.400	2.288	2.286	2.292	2.311	2.372	2.346
0.500	2.317	2.309	2.318	2.333	2.421	2.395
0.600	2.355	2.334	2.342	2.361	2.463	2.464
0.700	2.416	2.376	2.373	2.390	2.510	2.536
0.800	2.506	2.450	2.424	2.426	2.578	2.603
0.850	2.599	2.510	2.455	2.448	2.634	2.647
0.900	2.758	2.634	2.509	2.483	2.728	2.725
0.925	2.956	2.732	2.543	2.507	2.805	2.807
0.930	2.991	2.758	2.549	2.511	2.825	2.817
0.950	3.277	2.911	2.607	2.547	3.020	2.912
0.960	3.475	3.039	2.678	2.576	3.113	3.002
0.975	4.041	3.324	2.885	2.666	3.381	3.262
0.980	4.265	3.452	3.010	2.755	3.462	3.395
0.990	5.160	3.944	3.553	3.147	3.824	3.943

Table 4 (Cont'd). Cumulative Distributions of Zenith Atmospheric Noise Temperature at X-Band for Goldstone DSCC, K

CD	July	August	September	October	November	December	Minimum	Year Average	Maximum
0.000	2.135	2.135	2.135	2.135	2.135	2.135	2.135	2.135	2.135
0.100	2.294	2.306	2.332	2.268	2.227	2.207	2.207	2.251	2.332
0.200	2.365	2.375	2.374	2.303	2.262	2.239	2.238	2.291	2.375
0.250	2.387	2.402	2.393	2.315	2.274	2.248	2.248	2.305	2.402
0.300	2.422	2.447	2.425	2.336	2.292	2.263	2.263	2.327	2.447
0.400	2.474	2.512	2.481	2.375	2.325	2.284	2.284	2.362	2.512
0.500	2.545	2.592	2.553	2.408	2.366	2.307	2.307	2.405	2.592
0.600	2.630	2.652	2.612	2.444	2.426	2.335	2.334	2.451	2.652
0.700	2.739	2.695	2.690	2.488	2.487	2.382	2.373	2.507	2.739
0.800	2.830	2.760	2.766	2.552	2.556	2.460	2.424	2.576	2.830
0.850	2.878	2.805	2.813	2.600	2.603	2.541	2.448	2.628	2.878
0.900	2.946	2.876	2.915	2.681	2.680	2.676	2.483	2.718	2.946
0.925	2.996	2.924	2.981	2.725	2.726	2.773	2.507	2.790	2.996
0.930	3.009	2.934	2.989	2.732	2.731	2.801	2.511	2.804	3.009
0.950	3.074	3.019	3.066	2.793	2.777	3.048	2.547	2.921	3.277
0.960	3.126	3.078	3.141	2.850	2.824	3.208	2.576	3.009	3.475
0.975	3.295	3.246	3.356	3.022	2.963	3.631	2.666	3.256	4.041
0.980	3.404	3.272	3.577	3.120	3.098	3.819	2.755	3.386	4.265
0.990	3.912	3.377	4.578	3.585	3.663	4.570	3.147	3.938	5.160

Table 5. Cumulative Distributions of Zenith Atmospheric Noise Temperature at X-Band for Canberra DSCC, K

CD	January	February	March	April	May	June
0.000	2.327	2.327	2.327	2.327	2.327	2.327
0.100	2.631	2.741	2.815	2.607	2.531	2.513
0.200	2.725	2.841	2.895	2.679	2.568	2.594
0.250	2.763	2.892	2.924	2.705	2.587	2.612
0.300	2.792	2.948	2.953	2.732	2.607	2.626
0.400	2.853	3.057	3.021	2.783	2.641	2.656
0.500	2.955	3.162	3.087	2.843	2.678	2.691
0.600	3.057	3.287	3.187	2.902	2.714	2.730
0.700	3.177	3.439	3.303	2.978	2.782	2.777
0.800	3.321	3.641	3.433	3.101	2.974	2.849
0.850	3.419	3.848	3.527	3.198	3.112	2.918
0.900	3.604	4.396	3.704	3.385	3.387	3.063
0.925	3.780	4.829	3.898	3.687	3.738	3.299
0.930	3.821	4.921	3.963	3.757	3.848	3.401
0.950	4.138	5.483	4.287	4.109	4.399	3.929
0.960	4.361	5.843	4.465	4.366	4.802	4.164
0.975	5.027	6.950	4.966	5.062	5.740	4.695
0.980	5.435	7.580	5.350	5.412	5.997	4.965
0.990	7.589	9.469	6.492	6.392	7.091	5.622

Table 5 (Cont'd). Cumulative Distributions of Zenith Atmospheric Noise Temperature at X-Band for Canberra DSCC, K

CD	July	August	September	October	November	December	Minimum	Year Average	Maximum
0.000	2.327	2.327	2.327	2.327	2.327	2.327	2.327	2.327	2.327
0.100	2.485	2.491	2.548	2.550	2.649	2.562	2.485	2.594	2.815
0.200	2.532	2.539	2.600	2.617	2.723	2.648	2.532	2.663	2.895
0.250	2.551	2.556	2.621	2.640	2.755	2.693	2.551	2.692	2.924
0.300	2.567	2.570	2.643	2.662	2.790	2.731	2.567	2.718	2.953
0.400	2.598	2.598	2.688	2.705	2.858	2.801	2.598	2.772	3.057
0.500	2.636	2.628	2.732	2.760	2.924	2.871	2.628	2.831	3.162
0.600	2.676	2.669	2.785	2.837	3.002	2.958	2.669	2.900	3.287
0.700	2.725	2.723	2.863	2.942	3.117	3.079	2.723	2.992	3.439
0.800	2.823	2.807	2.966	3.153	3.362	3.298	2.807	3.144	3.641
0.850	2.907	2.900	3.062	3.310	3.594	3.501	2.900	3.275	3.848
0.900	3.045	3.125	3.232	3.625	3.955	3.834	3.045	3.530	4.396
0.925	3.222	3.351	3.396	3.982	4.312	4.131	3.222	3.802	4.829
0.930	3.265	3.413	3.464	4.077	4.403	4.234	3.265	3.881	4.921
0.950	3.484	3.741	3.852	4.704	4.938	4.690	3.484	4.313	5.483
0.960	3.649	4.037	4.146	5.064	5.266	4.920	3.649	4.590	5.843
0.975	3.999	5.018	4.766	6.097	6.453	5.522	3.999	5.358	6.950
0.980	4.187	5.340	5.165	6.757	7.003	5.794	4.187	5.749	7.580
0.990	4.874	6.481	6.882	8.346	8.552	6.732	4.874	7.043	9.469

Table 6. Cumulative Distributions of Zenith Atmospheric Noise Temperature at X-Band for Madrid DSCC, K

CD	January	February	March	April	May	June
0.000	2.239	2.239	2.239	2.239	2.239	2.239
0.100	2.314	2.310	2.378	2.386	2.483	2.522
0.200	2.364	2.358	2.425	2.442	2.545	2.585
0.250	2.379	2.372	2.442	2.456	2.564	2.604
0.300	2.401	2.392	2.466	2.475	2.592	2.634
0.400	2.439	2.423	2.502	2.512	2.639	2.677
0.500	2.492	2.470	2.551	2.561	2.679	2.722
0.600	2.565	2.524	2.605	2.620	2.723	2.767
0.700	2.695	2.588	2.684	2.700	2.775	2.816
0.800	3.013	2.697	2.829	2.859	2.897	2.877
0.850	3.365	2.855	2.984	3.019	3.137	2.922
0.900	4.006	3.167	3.322	3.264	3.662	3.004
0.925	4.714	3.499	3.697	3.506	4.213	3.074
0.930	4.835	3.567	3.773	3.562	4.320	3.095
0.950	5.796	4.089	4.239	4.047	4.971	3.280
0.960	6.151	4.379	4.536	4.328	5.324	3.452
0.975	6.990	5.186	5.323	4.965	6.142	4.021
0.980	7.242	5.454	5.623	5.155	6.438	4.411
0.990	8.190	6.491	6.646	5.847	7.435	5.921

Table 6 (Cont'd). Cumulative Distributions of Zenith Atmospheric Noise Temperature at X-Band for Madrid DSCC, K

CD	July	August	September	October	November	December	Minimum	Year Average	Maximum
0.000	2.239	2.239	2.239	2.239	2.239	2.239	2.239	2.239	2.239
0.100	2.560	2.563	2.519	2.442	2.235	2.312	2.235	2.419	2.563
0.200	2.618	2.626	2.588	2.542	2.373	2.375	2.358	2.487	2.626
0.250	2.636	2.645	2.611	2.571	2.397	2.398	2.372	2.506	2.645
0.300	2.662	2.674	2.646	2.616	2.436	2.436	2.392	2.536	2.674
0.400	2.704	2.717	2.699	2.688	2.483	2.500	2.423	2.582	2.717
0.500	2.744	2.760	2.754	2.765	2.538	2.565	2.470	2.633	2.765
0.600	2.784	2.806	2.814	2.855	2.615	2.649	2.524	2.694	2.855
0.700	2.825	2.851	2.874	2.972	2.717	2.794	2.588	2.774	2.972
0.800	2.873	2.910	2.951	3.241	2.910	3.114	2.697	2.931	3.241
0.850	2.902	2.943	3.002	3.544	3.196	3.461	2.855	3.111	3.544
0.900	2.948	2.997	3.095	4.108	3.757	4.037	2.948	3.447	4.108
0.925	2.981	3.029	3.196	4.674	4.342	4.572	2.981	3.791	4.714
0.930	2.987	3.036	3.218	4.779	4.438	4.650	2.987	3.855	4.835
0.950	3.034	3.086	3.414	5.576	5.212	5.289	3.034	4.336	5.796
0.960	3.064	3.125	3.614	5.940	5.540	5.592	3.064	4.587	6.151
0.975	3.168	3.253	4.272	6.842	6.389	6.380	3.168	5.244	6.990
0.980	3.257	3.344	4.769	7.208	6.619	6.624	3.257	5.512	7.242
0.990	3.702	3.734	6.609	8.606	7.512	7.475	3.702	6.514	8.606

Table 7. Cumulative Distributions of Zenith Atmospheric Noise Temperature at Ka-Band for Goldstone DSCC, K

CD	January	February	March	April	May	June
0.000	6.700	6.700	6.700	6.700	6.700	6.700
0.100	7.904	7.785	7.925	8.119	8.463	8.302
0.200	8.227	8.181	8.321	8.594	9.041	8.856
0.250	8.354	8.342	8.441	8.731	9.233	9.031
0.300	8.564	8.563	8.626	8.948	9.531	9.304
0.400	8.915	8.888	8.967	9.237	10.127	9.748
0.500	9.325	9.218	9.346	9.563	10.837	10.450
0.600	9.870	9.575	9.688	9.962	11.441	11.447
0.700	10.764	10.181	10.134	10.383	12.115	12.488
0.800	12.058	11.252	10.868	10.909	13.100	13.459
0.850	13.395	12.119	11.316	11.226	13.912	14.098
0.900	15.703	13.903	12.100	11.726	15.260	15.217
0.925	18.556	15.328	12.600	12.070	16.383	16.399
0.930	19.068	15.702	12.683	12.133	16.670	16.548
0.950	23.198	17.912	13.523	12.651	19.479	17.919
0.960	26.054	19.756	14.550	13.068	20.820	19.226
0.975	34.229	23.875	17.527	14.366	24.702	22.976
0.980	37.463	25.724	19.338	15.656	25.866	24.904
0.990	50.394	32.834	27.182	21.314	31.090	32.814

Table 7 (Cont'd). Cumulative Distributions of Zenith Atmospheric Noise Temperature at Ka-Band for Goldstone DSCC, K

CD	July	August	September	October	November	December	Minimum	Year Average	Maximum
0.000	6.700	6.700	6.700	6.700	6.700	6.700	6.700	6.700	6.700
0.100	8.999	9.167	9.539	8.617	8.028	7.746	7.746	8.383	9.539
0.200	10.021	10.163	10.153	9.130	8.529	8.197	8.181	8.951	10.163
0.250	10.341	10.559	10.424	9.301	8.701	8.337	8.337	9.150	10.559
0.300	10.848	11.213	10.890	9.606	8.969	8.549	8.549	9.468	11.213
0.400	11.592	12.143	11.701	10.170	9.444	8.854	8.854	9.982	12.143
0.500	12.618	13.303	12.736	10.649	10.037	9.186	9.186	10.606	13.303
0.600	13.848	14.174	13.595	11.156	10.899	9.585	9.575	11.270	14.174
0.700	15.424	14.787	14.714	11.805	11.782	10.264	10.134	12.070	15.424
0.800	16.742	15.727	15.812	12.722	12.786	11.389	10.868	13.069	16.742
0.850	17.426	16.371	16.487	13.410	13.465	12.566	11.226	13.816	17.426
0.900	18.419	17.398	17.964	14.581	14.576	14.521	11.726	15.114	18.419
0.925	19.131	18.090	18.919	15.220	15.229	15.921	12.070	16.154	19.131
0.930	19.323	18.247	19.040	15.317	15.304	16.325	12.133	16.363	19.323
0.950	20.260	19.474	20.152	16.204	15.976	19.884	12.651	18.053	23.198
0.960	21.008	20.321	21.234	17.020	16.651	22.199	13.068	19.326	26.054
0.975	23.451	22.752	24.331	19.512	18.657	28.306	14.366	22.890	34.229
0.980	25.032	23.123	27.535	20.927	20.607	31.025	15.656	24.767	37.463
0.990	32.362	24.643	41.986	27.647	28.774	41.871	21.314	32.743	50.394

Table 8. Cumulative Distributions of Zenith Atmospheric Noise Temperature at Ka-Band for Canberra DSCC, K

CD	January	February	March	April	May	June
0.000	7.274	7.274	7.274	7.274	7.274	7.274
0.100	11.671	13.259	14.320	11.313	10.215	9.957
0.200	13.019	14.694	15.485	12.360	10.760	11.133
0.250	13.570	15.432	15.895	12.740	11.030	11.390
0.300	13.996	16.240	16.314	13.120	11.320	11.594
0.400	14.873	17.813	17.305	13.865	11.810	12.023
0.500	16.347	19.333	18.255	14.730	12.340	12.530
0.600	17.820	21.135	19.690	15.580	12.870	13.093
0.700	19.554	23.330	21.375	16.675	13.844	13.780
0.800	21.631	26.251	23.250	18.455	16.624	14.809
0.850	23.048	29.237	24.613	19.853	18.614	15.805
0.900	25.721	37.155	27.169	22.553	22.586	17.897
0.925	28.258	43.415	29.972	26.919	27.655	21.311
0.930	28.846	44.748	30.911	27.935	29.242	22.786
0.950	33.438	52.852	35.590	33.007	37.206	30.415
0.960	36.657	58.057	38.148	36.725	43.020	33.801
0.975	46.274	74.052	45.395	46.781	56.575	41.481
0.980	52.169	83.148	50.943	51.827	60.285	45.372
0.990	83.280	110.437	67.432	65.986	76.082	54.859

Table 8 (Cont'd). Cumulative Distributions of Zenith Atmospheric Noise Temperature at Ka-Band for Canberra DSCC, K

CD	July	August	September	October	November	December	Minimum	Year Average	Maximum
0.000	7.274	7.274	7.274	7.274	7.274	7.274	7.274	7.274	7.274
0.100	9.563	9.638	10.470	10.500	11.923	10.670	9.563	11.125	14.320
0.200	10.235	10.333	11.213	11.467	12.993	11.917	10.235	12.134	15.485
0.250	10.505	10.580	11.523	11.800	13.452	12.553	10.505	12.539	15.895
0.300	10.743	10.789	11.840	12.113	13.957	13.103	10.743	12.927	16.314
0.400	11.188	11.190	12.493	12.737	14.940	14.117	11.188	13.696	17.813
0.500	11.730	11.619	13.128	13.533	15.893	15.133	11.619	14.548	19.333
0.600	12.313	12.215	13.887	14.633	17.030	16.381	12.215	15.554	21.135
0.700	13.028	12.988	15.017	16.155	18.682	18.143	12.988	16.881	23.330
0.800	14.442	14.200	16.511	19.203	22.224	21.303	14.200	19.075	26.251
0.850	15.655	15.547	17.889	21.470	25.576	24.236	15.547	20.962	29.237
0.900	17.645	18.804	20.349	26.021	30.782	29.038	17.645	24.643	37.155
0.925	20.202	22.063	22.720	31.181	35.946	33.327	20.202	28.581	43.415
0.930	20.824	22.967	23.690	32.545	37.255	34.818	20.824	29.714	44.748
0.950	23.988	27.691	29.298	41.607	44.979	41.402	23.988	35.956	52.852
0.960	26.372	31.975	33.550	46.812	49.729	44.727	26.372	39.964	58.057
0.975	31.422	46.147	42.500	61.731	66.869	53.428	31.422	51.054	74.052
0.980	34.134	50.786	48.262	71.255	74.809	57.345	34.134	56.695	83.148
0.990	44.061	67.266	73.060	94.217	97.186	70.896	44.061	75.397	110.437

Table 9. Cumulative Distributions of Zenith Atmospheric Noise Temperature at Ka-Band for Madrid DSCC, K

CD	January	February	March	April	May	June
0.000	7.000	7.000	7.000	7.000	7.000	7.000
0.100	8.081	8.027	9.008	9.129	10.527	11.095
0.200	8.807	8.715	9.680	9.934	11.424	12.001
0.250	9.020	8.918	9.928	10.128	11.700	12.279
0.300	9.345	9.209	10.275	10.413	12.094	12.701
0.400	9.893	9.661	10.801	10.941	12.778	13.321
0.500	10.660	10.343	11.505	11.649	13.349	13.978
0.600	11.705	11.122	12.284	12.505	13.985	14.626
0.700	13.588	12.034	13.426	13.658	14.740	15.331
0.800	18.184	13.617	15.527	15.956	16.508	16.218
0.850	23.264	15.894	17.764	18.261	19.967	16.865
0.900	32.518	20.404	22.635	21.803	27.555	18.056
0.925	42.747	25.199	28.054	25.304	35.506	19.059
0.930	44.501	26.176	29.154	26.115	37.057	19.361
0.950	58.380	33.714	35.887	33.118	46.457	22.041
0.960	63.503	37.904	40.178	37.171	51.554	24.514
0.975	75.622	49.567	51.540	46.376	63.371	32.733
0.980	79.259	53.436	55.884	49.123	67.655	38.373
0.990	92.957	68.414	70.648	59.108	82.045	60.183

Table 9 (Cont'd). Cumulative Distributions of Zenith Atmospheric Noise Temperature at Ka-Band for Madrid DSCC, K

CD	July	August	September	October	November	December	Minimum	Year Average	Maximum
0.000	7.000	7.000	7.000	7.000	7.000	7.000	7.000	7.000	7.000
0.100	11.629	11.685	11.048	9.928	6.945	8.053	6.945	9.596	11.685
0.200	12.472	12.584	12.045	11.382	8.940	8.957	8.715	10.578	12.584
0.250	12.729	12.868	12.368	11.802	9.280	9.297	8.918	10.860	12.868
0.300	13.108	13.287	12.877	12.451	9.852	9.845	9.209	11.288	13.287
0.400	13.719	13.901	13.650	13.489	10.522	10.775	9.661	11.954	13.901
0.500	14.290	14.523	14.437	14.599	11.318	11.708	10.343	12.697	14.599
0.600	14.866	15.183	15.311	15.893	12.425	12.920	11.122	13.569	15.893
0.700	15.470	15.844	16.170	17.581	13.910	15.023	12.034	14.731	17.581
0.800	16.164	16.691	17.282	21.475	16.699	19.634	13.617	16.996	21.475
0.850	16.577	17.169	18.017	25.853	20.829	24.646	15.894	19.592	25.853
0.900	17.245	17.946	19.369	33.998	28.929	32.965	17.245	24.452	33.998
0.925	17.715	18.413	20.820	42.171	37.379	40.700	17.715	29.422	42.747
0.930	17.803	18.505	21.142	43.694	38.756	41.828	17.803	30.341	44.501
0.950	18.487	19.229	23.978	55.198	49.934	51.055	18.487	37.290	58.380
0.960	18.918	19.803	26.856	60.459	54.681	55.436	18.918	40.915	63.503
0.975	20.416	21.652	36.364	73.478	66.936	66.807	20.416	50.405	75.622
0.980	21.709	22.960	43.548	78.764	70.263	70.341	21.709	54.276	79.259
0.990	28.129	28.596	70.125	98.968	83.164	82.632	28.129	68.747	98.968

Table 10. Cumulative Distributions of Zenith Atmospheric Attenuation at L- and S-Bands for Goldstone DSCC, dB

CD	January	February	March	April	May	June
0.000	0.033	0.033	0.033	0.033	0.033	0.033
0.100	0.033	0.033	0.033	0.033	0.033	0.033
0.200	0.032	0.032	0.032	0.032	0.032	0.032
0.250	0.032	0.032	0.032	0.032	0.032	0.032
0.300	0.032	0.032	0.032	0.032	0.032	0.032
0.400	0.032	0.032	0.032	0.032	0.032	0.032
0.500	0.031	0.031	0.031	0.031	0.032	0.032
0.600	0.031	0.031	0.031	0.031	0.031	0.031
0.700	0.031	0.031	0.031	0.031	0.031	0.031
0.800	0.031	0.031	0.031	0.031	0.031	0.031
0.850	0.031	0.031	0.031	0.031	0.031	0.031
0.900	0.031	0.031	0.031	0.031	0.031	0.031
0.925	0.031	0.031	0.031	0.030	0.031	0.031
0.930	0.031	0.031	0.031	0.030	0.031	0.031
0.950	0.031	0.031	0.031	0.030	0.031	0.031
0.960	0.032	0.031	0.031	0.030	0.031	0.031
0.975	0.032	0.031	0.031	0.031	0.031	0.031
0.980	0.032	0.031	0.031	0.031	0.031	0.031
0.990	0.033	0.032	0.032	0.031	0.032	0.032

Table 10 (Cont'd). Cumulative Distributions of Zenith Atmospheric Attenuation at L- and S-Bands for Goldstone DSCC, dB

CD	July	August	September	October	November	December	Minimum	Year Average	Maximum
0.000	0.033	0.033	0.033	0.033	0.033	0.033	0.033	0.033	0.033
0.100	0.033	0.033	0.033	0.033	0.033	0.033	0.033	0.033	0.033
0.200	0.032	0.032	0.032	0.032	0.032	0.032	0.032	0.032	0.032
0.250	0.032	0.032	0.032	0.032	0.032	0.032	0.032	0.032	0.032
0.300	0.032	0.032	0.032	0.032	0.032	0.032	0.032	0.032	0.032
0.400	0.032	0.032	0.032	0.032	0.032	0.032	0.032	0.032	0.032
0.500	0.032	0.032	0.032	0.032	0.032	0.031	0.031	0.032	0.032
0.600	0.032	0.032	0.032	0.031	0.031	0.031	0.031	0.031	0.032
0.700	0.031	0.031	0.031	0.031	0.031	0.031	0.031	0.031	0.031
0.800	0.031	0.031	0.031	0.031	0.031	0.031	0.031	0.031	0.031
0.850	0.031	0.031	0.031	0.031	0.031	0.031	0.031	0.031	0.031
0.900	0.031	0.031	0.031	0.031	0.031	0.031	0.031	0.031	0.031
0.925	0.031	0.031	0.031	0.031	0.031	0.031	0.030	0.031	0.031
0.930	0.031	0.031	0.031	0.031	0.031	0.031	0.030	0.031	0.031
0.950	0.031	0.031	0.031	0.031	0.031	0.031	0.030	0.031	0.031
0.960	0.031	0.031	0.031	0.031	0.031	0.031	0.030	0.031	0.032
0.975	0.031	0.031	0.031	0.031	0.031	0.032	0.031	0.031	0.032
0.980	0.031	0.031	0.032	0.031	0.031	0.032	0.031	0.031	0.032
0.990	0.032	0.031	0.033	0.032	0.032	0.033	0.031	0.032	0.033

Table 11. Cumulative Distributions of Zenith Atmospheric Attenuation at L- and S-Bands for Canberra DSCC, dB

CD	January	February	March	April	May	June
0.000	0.036	0.036	0.036	0.036	0.036	0.036
0.100	0.036	0.036	0.036	0.036	0.036	0.036
0.200	0.035	0.036	0.036	0.035	0.035	0.035
0.250	0.035	0.036	0.036	0.035	0.035	0.035
0.300	0.035	0.035	0.035	0.035	0.035	0.035
0.400	0.035	0.035	0.035	0.035	0.035	0.035
0.500	0.035	0.035	0.035	0.035	0.034	0.034
0.600	0.035	0.035	0.035	0.034	0.034	0.034
0.700	0.034	0.035	0.035	0.034	0.034	0.034
0.800	0.034	0.035	0.034	0.034	0.034	0.034
0.850	0.034	0.035	0.034	0.034	0.034	0.034
0.900	0.034	0.035	0.034	0.034	0.034	0.034
0.925	0.034	0.036	0.035	0.034	0.034	0.034
0.930	0.034	0.036	0.035	0.034	0.034	0.034
0.950	0.035	0.036	0.035	0.035	0.035	0.034
0.960	0.035	0.037	0.035	0.035	0.035	0.035
0.975	0.036	0.038	0.036	0.036	0.037	0.035
0.980	0.036	0.039	0.036	0.036	0.037	0.036
0.990	0.039	0.041	0.037	0.037	0.038	0.036

Table 11 (Cont'd). Cumulative Distributions of Zenith Atmospheric Attenuation at L- and S-Bands for Canberra DSCC, dB

CD	July	August	September	October	November	December	Minimum	Year Average	Maximum
0.000	0.036	0.036	0.036	0.036	0.036	0.036	0.036	0.036	0.036
0.100	0.036	0.036	0.036	0.036	0.036	0.036	0.036	0.036	0.036
0.200	0.035	0.035	0.035	0.035	0.035	0.035	0.035	0.035	0.036
0.250	0.035	0.035	0.035	0.035	0.035	0.035	0.035	0.035	0.036
0.300	0.035	0.035	0.035	0.035	0.035	0.035	0.035	0.035	0.035
0.400	0.035	0.035	0.035	0.035	0.035	0.035	0.035	0.035	0.035
0.500	0.034	0.034	0.034	0.035	0.035	0.035	0.034	0.035	0.035
0.600	0.034	0.034	0.034	0.034	0.034	0.034	0.034	0.034	0.035
0.700	0.034	0.034	0.034	0.034	0.034	0.034	0.034	0.034	0.035
0.800	0.034	0.034	0.034	0.034	0.034	0.034	0.034	0.034	0.035
0.850	0.034	0.034	0.034	0.034	0.034	0.034	0.034	0.034	0.035
0.900	0.034	0.034	0.034	0.034	0.035	0.035	0.034	0.034	0.035
0.925	0.034	0.034	0.034	0.035	0.035	0.035	0.034	0.034	0.036
0.930	0.034	0.034	0.034	0.035	0.035	0.035	0.034	0.034	0.036
0.950	0.034	0.034	0.034	0.035	0.036	0.035	0.034	0.035	0.036
0.960	0.034	0.035	0.035	0.036	0.036	0.036	0.034	0.035	0.037
0.975	0.034	0.036	0.035	0.037	0.037	0.036	0.034	0.036	0.038
0.980	0.035	0.036	0.036	0.038	0.038	0.037	0.035	0.037	0.039
0.990	0.035	0.037	0.038	0.039	0.040	0.038	0.035	0.038	0.041

Table 12. Cumulative Distributions of Zenith Atmospheric Attenuation at L- and S-Bands for Madrid DSCC, dB

CD	January	February	March	April	May	June
0.000	0.034	0.034	0.034	0.034	0.034	0.034
0.100	0.034	0.034	0.034	0.034	0.034	0.034
0.200	0.034	0.034	0.034	0.034	0.034	0.034
0.250	0.034	0.034	0.034	0.034	0.034	0.034
0.300	0.034	0.034	0.034	0.034	0.034	0.034
0.400	0.033	0.033	0.033	0.033	0.034	0.034
0.500	0.033	0.033	0.033	0.033	0.033	0.033
0.600	0.033	0.033	0.033	0.033	0.033	0.033
0.700	0.033	0.033	0.033	0.033	0.033	0.033
0.800	0.033	0.032	0.033	0.033	0.033	0.033
0.850	0.033	0.032	0.033	0.033	0.033	0.032
0.900	0.034	0.033	0.033	0.033	0.033	0.032
0.925	0.034	0.033	0.033	0.033	0.034	0.032
0.930	0.034	0.033	0.033	0.033	0.034	0.032
0.950	0.036	0.034	0.034	0.034	0.035	0.033
0.960	0.036	0.034	0.034	0.034	0.035	0.033
0.975	0.037	0.035	0.035	0.034	0.036	0.033
0.980	0.037	0.035	0.035	0.035	0.036	0.034
0.990	0.038	0.036	0.036	0.035	0.037	0.036

Table 12 (Cont'd). Cumulative Distributions of Zenith Atmospheric Attenuation at L- and S-Bands for Madrid DSCC, dB

CD	July	August	September	October	November	December	Minimum	Maximum	Year Average
0.000	0.034	0.034	0.034	0.034	0.034	0.034	0.034	0.034	0.034
0.100	0.034	0.034	0.034	0.034	0.034	0.034	0.034	0.034	0.034
0.200	0.034	0.034	0.034	0.034	0.034	0.034	0.034	0.034	0.034
0.250	0.034	0.034	0.034	0.034	0.034	0.034	0.034	0.034	0.034
0.300	0.034	0.034	0.034	0.034	0.034	0.034	0.034	0.034	0.034
0.400	0.034	0.034	0.034	0.034	0.033	0.033	0.033	0.033	0.034
0.500	0.033	0.033	0.033	0.033	0.033	0.033	0.033	0.033	0.033
0.600	0.033	0.033	0.033	0.033	0.033	0.033	0.033	0.033	0.033
0.700	0.033	0.033	0.033	0.033	0.033	0.033	0.033	0.033	0.033
0.800	0.033	0.033	0.033	0.033	0.033	0.033	0.032	0.033	0.033
0.850	0.032	0.033	0.033	0.033	0.033	0.033	0.032	0.033	0.033
0.900	0.032	0.032	0.033	0.034	0.033	0.034	0.032	0.033	0.034
0.925	0.032	0.032	0.033	0.034	0.034	0.034	0.032	0.033	0.034
0.930	0.032	0.032	0.033	0.034	0.034	0.034	0.032	0.033	0.034
0.950	0.032	0.032	0.033	0.035	0.035	0.035	0.032	0.034	0.036
0.960	0.032	0.032	0.033	0.036	0.035	0.035	0.032	0.034	0.036
0.975	0.032	0.033	0.034	0.037	0.036	0.036	0.032	0.035	0.037
0.980	0.032	0.033	0.034	0.037	0.036	0.036	0.032	0.035	0.037
0.990	0.033	0.033	0.036	0.039	0.037	0.037	0.033	0.036	0.039

Table 13. Cumulative Distributions of Zenith Atmospheric Attenuation at X-Band
for Goldstone DSCC, dB

CD	January	February	March	April	May	June
0.000	0.037	0.037	0.037	0.037	0.037	0.037
0.100	0.038	0.037	0.038	0.038	0.038	0.038
0.200	0.038	0.038	0.038	0.038	0.039	0.038
0.250	0.038	0.038	0.038	0.038	0.039	0.038
0.300	0.038	0.038	0.038	0.038	0.039	0.038
0.400	0.038	0.038	0.038	0.038	0.039	0.039
0.500	0.038	0.038	0.038	0.038	0.039	0.039
0.600	0.038	0.038	0.038	0.038	0.040	0.040
0.700	0.039	0.038	0.038	0.038	0.040	0.041
0.800	0.040	0.039	0.038	0.038	0.041	0.041
0.850	0.041	0.040	0.039	0.039	0.042	0.042
0.900	0.043	0.041	0.039	0.039	0.043	0.043
0.925	0.046	0.043	0.040	0.039	0.044	0.044
0.930	0.047	0.043	0.040	0.039	0.044	0.044
0.950	0.051	0.046	0.041	0.040	0.047	0.046
0.960	0.054	0.048	0.042	0.040	0.049	0.047
0.975	0.063	0.052	0.045	0.042	0.053	0.051
0.980	0.067	0.054	0.047	0.043	0.054	0.053
0.990	0.081	0.062	0.056	0.049	0.060	0.062

Table 13 (Cont'd). Cumulative Distributions of Zenith Atmospheric Attenuation at X-Band
for Goldstone DSCC, dB

CD	July	August	September	October	November	December	Minimum	Year Average	Maximum
0.000	0.037	0.037	0.037	0.037	0.037	0.037	0.037	0.037	0.037
0.100	0.039	0.039	0.040	0.038	0.038	0.037	0.037	0.038	0.040
0.200	0.040	0.040	0.040	0.039	0.038	0.038	0.038	0.038	0.040
0.250	0.040	0.040	0.040	0.039	0.038	0.038	0.038	0.038	0.040
0.300	0.040	0.041	0.040	0.039	0.038	0.038	0.038	0.039	0.041
0.400	0.041	0.041	0.041	0.039	0.038	0.038	0.038	0.039	0.041
0.500	0.042	0.042	0.042	0.039	0.039	0.038	0.038	0.039	0.042
0.600	0.043	0.043	0.042	0.039	0.039	0.038	0.038	0.040	0.043
0.700	0.044	0.043	0.043	0.040	0.040	0.038	0.038	0.040	0.044
0.800	0.045	0.044	0.044	0.040	0.041	0.039	0.038	0.041	0.045
0.850	0.045	0.044	0.044	0.041	0.041	0.040	0.039	0.042	0.045
0.900	0.046	0.045	0.046	0.042	0.042	0.042	0.039	0.043	0.046
0.925	0.047	0.046	0.047	0.043	0.043	0.044	0.039	0.044	0.047
0.930	0.047	0.046	0.047	0.043	0.043	0.044	0.039	0.044	0.047
0.950	0.048	0.047	0.048	0.044	0.043	0.048	0.040	0.046	0.051
0.960	0.049	0.048	0.049	0.045	0.044	0.050	0.040	0.047	0.054
0.975	0.052	0.051	0.052	0.047	0.046	0.057	0.042	0.051	0.063
0.980	0.053	0.051	0.056	0.049	0.048	0.060	0.043	0.053	0.067
0.990	0.061	0.053	0.072	0.056	0.057	0.072	0.049	0.062	0.081

Table 14. Cumulative Distributions of Zenith Atmospheric Attenuation at X-Band
for Canberra DSCC, dB

CD	January	February	March	April	May	June
0.000	0.040	0.040	0.040	0.040	0.040	0.040
0.100	0.045	0.046	0.048	0.044	0.043	0.043
0.200	0.046	0.048	0.049	0.045	0.043	0.044
0.250	0.046	0.048	0.049	0.045	0.043	0.044
0.300	0.046	0.049	0.049	0.045	0.043	0.044
0.400	0.047	0.050	0.050	0.046	0.043	0.044
0.500	0.048	0.052	0.050	0.046	0.044	0.044
0.600	0.049	0.053	0.052	0.047	0.044	0.044
0.700	0.051	0.055	0.053	0.048	0.045	0.044
0.800	0.053	0.058	0.055	0.049	0.047	0.045
0.850	0.054	0.061	0.056	0.051	0.049	0.046
0.900	0.057	0.069	0.058	0.053	0.053	0.048
0.925	0.059	0.076	0.061	0.058	0.059	0.052
0.930	0.060	0.078	0.062	0.059	0.060	0.053
0.950	0.065	0.086	0.067	0.064	0.069	0.062
0.960	0.068	0.092	0.070	0.068	0.075	0.065
0.975	0.079	0.109	0.078	0.079	0.090	0.074
0.980	0.085	0.119	0.084	0.085	0.094	0.078
0.990	0.119	0.150	0.102	0.100	0.112	0.088

Table 14 (Cont'd). Cumulative Distributions of Zenith Atmospheric Attenuation at X-Band
for Canberra DSCC, dB

CD	July	August	September	October	November	December	Minimum	Year Average	Maximum
0.000	0.040	0.040	0.040	0.040	0.040	0.040	0.040	0.040	0.040
0.100	0.042	0.042	0.043	0.043	0.045	0.043	0.042	0.044	0.048
0.200	0.043	0.043	0.044	0.044	0.046	0.044	0.043	0.045	0.049
0.250	0.043	0.043	0.044	0.044	0.046	0.045	0.043	0.045	0.049
0.300	0.043	0.043	0.044	0.044	0.046	0.045	0.043	0.045	0.049
0.400	0.043	0.043	0.044	0.045	0.047	0.046	0.043	0.046	0.050
0.500	0.043	0.043	0.045	0.045	0.048	0.047	0.043	0.046	0.052
0.600	0.043	0.043	0.045	0.046	0.049	0.048	0.043	0.047	0.053
0.700	0.044	0.044	0.046	0.047	0.050	0.049	0.044	0.048	0.055
0.800	0.045	0.045	0.047	0.050	0.053	0.052	0.045	0.050	0.058
0.850	0.046	0.046	0.048	0.052	0.057	0.055	0.046	0.052	0.061
0.900	0.048	0.049	0.051	0.057	0.062	0.060	0.048	0.056	0.069
0.925	0.051	0.053	0.053	0.063	0.068	0.065	0.051	0.060	0.076
0.930	0.051	0.054	0.054	0.064	0.069	0.067	0.051	0.061	0.078
0.950	0.055	0.059	0.060	0.074	0.078	0.074	0.055	0.068	0.086
0.960	0.057	0.063	0.065	0.080	0.083	0.077	0.057	0.072	0.092
0.975	0.063	0.079	0.075	0.096	0.101	0.087	0.063	0.084	0.109
0.980	0.066	0.084	0.081	0.106	0.110	0.091	0.066	0.090	0.119
0.990	0.076	0.102	0.108	0.132	0.135	0.106	0.076	0.111	0.150

Table 15. Cumulative Distributions of Zenith Atmospheric Attenuation at X-Band
for Madrid DSCC, dB

CD	January	February	March	April	May	June
0.000	0.038	0.038	0.038	0.038	0.038	0.038
0.100	0.039	0.039	0.040	0.040	0.042	0.043
0.200	0.040	0.040	0.041	0.041	0.043	0.043
0.250	0.040	0.040	0.041	0.041	0.043	0.044
0.300	0.040	0.040	0.041	0.041	0.043	0.044
0.400	0.040	0.040	0.041	0.041	0.043	0.044
0.500	0.041	0.040	0.042	0.042	0.044	0.044
0.600	0.041	0.041	0.042	0.042	0.044	0.045
0.700	0.043	0.041	0.043	0.043	0.044	0.045
0.800	0.048	0.043	0.045	0.045	0.046	0.046
0.850	0.053	0.045	0.047	0.048	0.050	0.046
0.900	0.063	0.050	0.052	0.051	0.058	0.047
0.925	0.074	0.055	0.058	0.055	0.066	0.048
0.930	0.076	0.056	0.059	0.056	0.068	0.049
0.950	0.091	0.064	0.067	0.064	0.078	0.051
0.960	0.097	0.069	0.071	0.068	0.084	0.054
0.975	0.110	0.081	0.084	0.078	0.097	0.063
0.980	0.114	0.086	0.088	0.081	0.101	0.069
0.990	0.129	0.102	0.104	0.092	0.117	0.093

Table 15 (Cont'd). Cumulative Distributions of Zenith Atmospheric Attenuation at X-Band
for Madrid DSCC, dB

CD	July	August	September	October	November	December	Minimum	Year Average	Maximum
0.000	0.038	0.038	0.038	0.038	0.038	0.038	0.038	0.038	0.038
0.100	0.043	0.043	0.043	0.041	0.038	0.039	0.038	0.041	0.043
0.200	0.044	0.044	0.043	0.043	0.040	0.040	0.040	0.042	0.044
0.250	0.044	0.044	0.044	0.043	0.040	0.040	0.040	0.042	0.044
0.300	0.044	0.044	0.044	0.044	0.040	0.040	0.040	0.042	0.044
0.400	0.045	0.045	0.044	0.044	0.041	0.041	0.040	0.043	0.045
0.500	0.045	0.045	0.045	0.045	0.041	0.042	0.040	0.043	0.045
0.600	0.045	0.045	0.046	0.046	0.042	0.043	0.041	0.044	0.046
0.700	0.045	0.046	0.046	0.048	0.044	0.045	0.041	0.044	0.048
0.800	0.046	0.046	0.047	0.051	0.046	0.049	0.043	0.047	0.051
0.850	0.046	0.047	0.047	0.056	0.051	0.055	0.045	0.049	0.056
0.900	0.046	0.047	0.049	0.065	0.059	0.064	0.046	0.054	0.065
0.925	0.047	0.048	0.050	0.074	0.068	0.072	0.047	0.060	0.074
0.930	0.047	0.048	0.051	0.075	0.070	0.073	0.047	0.061	0.076
0.950	0.048	0.048	0.054	0.088	0.082	0.083	0.048	0.068	0.091
0.960	0.048	0.049	0.057	0.093	0.087	0.088	0.048	0.072	0.097
0.975	0.050	0.051	0.067	0.108	0.100	0.100	0.050	0.082	0.110
0.980	0.051	0.052	0.075	0.113	0.104	0.104	0.051	0.087	0.114
0.990	0.058	0.058	0.104	0.136	0.118	0.118	0.058	0.102	0.136

Table 16. Cumulative Distributions of Zenith Atmospheric Attenuation at Ka-Band
for Goldstone DSCC, dB

CD	January	February	March	April	May	June
0.000	0.116	0.116	0.116	0.116	0.116	0.116
0.100	0.135	0.133	0.136	0.139	0.145	0.142
0.200	0.140	0.139	0.141	0.146	0.154	0.150
0.250	0.141	0.141	0.143	0.148	0.156	0.153
0.300	0.144	0.144	0.145	0.151	0.161	0.157
0.400	0.149	0.148	0.150	0.154	0.169	0.163
0.500	0.154	0.152	0.154	0.158	0.180	0.173
0.600	0.162	0.157	0.159	0.163	0.188	0.188
0.700	0.175	0.165	0.165	0.169	0.198	0.204
0.800	0.195	0.181	0.175	0.176	0.212	0.218
0.850	0.216	0.195	0.182	0.180	0.224	0.227
0.900	0.253	0.223	0.194	0.188	0.246	0.245
0.925	0.300	0.246	0.201	0.193	0.264	0.264
0.930	0.308	0.252	0.203	0.194	0.268	0.266
0.950	0.377	0.288	0.216	0.202	0.315	0.289
0.960	0.426	0.319	0.233	0.208	0.337	0.310
0.975	0.568	0.388	0.281	0.229	0.402	0.373
0.980	0.625	0.419	0.311	0.250	0.422	0.405
0.990	0.863	0.542	0.444	0.344	0.512	0.542

Table 16 (Cont'd). Cumulative Distributions of Zenith Atmospheric Attenuation at Ka-Band
for Goldstone DSCC, dB

CD	July	August	September	October	November	December	Minimum	Year Average	Maximum
0.000	0.116	0.116	0.116	0.116	0.116	0.116	0.116	0.116	0.116
0.100	0.154	0.157	0.164	0.148	0.138	0.133	0.133	0.144	0.164
0.200	0.171	0.173	0.173	0.155	0.145	0.139	0.139	0.152	0.173
0.250	0.175	0.179	0.177	0.157	0.147	0.141	0.141	0.155	0.179
0.300	0.183	0.190	0.184	0.162	0.151	0.144	0.144	0.160	0.190
0.400	0.194	0.204	0.196	0.170	0.158	0.148	0.148	0.167	0.204
0.500	0.210	0.222	0.212	0.176	0.166	0.152	0.152	0.176	0.222
0.600	0.229	0.234	0.224	0.183	0.179	0.157	0.157	0.185	0.234
0.700	0.253	0.242	0.241	0.192	0.192	0.167	0.165	0.197	0.253
0.800	0.273	0.256	0.257	0.206	0.207	0.184	0.175	0.211	0.273
0.850	0.283	0.265	0.267	0.216	0.217	0.202	0.180	0.223	0.283
0.900	0.298	0.281	0.291	0.234	0.234	0.233	0.188	0.243	0.298
0.925	0.309	0.292	0.306	0.244	0.245	0.256	0.193	0.260	0.309
0.930	0.313	0.295	0.308	0.246	0.246	0.263	0.194	0.263	0.313
0.950	0.328	0.315	0.326	0.260	0.256	0.321	0.202	0.291	0.377
0.960	0.340	0.328	0.344	0.273	0.267	0.360	0.208	0.312	0.426
0.975	0.381	0.369	0.396	0.314	0.300	0.464	0.229	0.371	0.568
0.980	0.407	0.375	0.450	0.338	0.333	0.511	0.250	0.403	0.625
0.990	0.534	0.400	0.706	0.452	0.471	0.704	0.344	0.541	0.863

Table 17. Cumulative Distributions of Zenith Atmospheric Attenuation at Ka-Band
for Canberra DSCC, dB

CD	January	February	March	April	May	June
0.000	0.126	0.126	0.126	0.126	0.126	0.126
0.100	0.201	0.230	0.248	0.195	0.176	0.171
0.200	0.223	0.253	0.267	0.212	0.184	0.190
0.250	0.232	0.264	0.273	0.217	0.187	0.194
0.300	0.238	0.277	0.279	0.223	0.191	0.196
0.400	0.251	0.302	0.293	0.233	0.198	0.202
0.500	0.274	0.326	0.307	0.246	0.205	0.208
0.600	0.297	0.354	0.329	0.258	0.212	0.216
0.700	0.323	0.389	0.355	0.274	0.226	0.225
0.800	0.356	0.436	0.384	0.302	0.271	0.240
0.850	0.378	0.486	0.405	0.324	0.303	0.256
0.900	0.422	0.624	0.447	0.368	0.369	0.290
0.925	0.465	0.737	0.495	0.442	0.455	0.346
0.930	0.475	0.761	0.511	0.459	0.482	0.371
0.950	0.555	0.913	0.593	0.547	0.622	0.502
0.960	0.612	1.013	0.639	0.613	0.727	0.561
0.975	0.786	1.337	0.770	0.796	0.983	0.698
0.980	0.897	1.533	0.874	0.891	1.055	0.769
0.990	1.535	2.181	1.198	1.168	1.378	0.948

Table 17 (Cont'd). Cumulative Distributions of Zenith Atmospheric Attenuation at Ka-Band
for Canberra DSCC, dB

CD	July	August	September	October	November	December	Minimum	Year Average	Maximum
0.000	0.126	0.126	0.126	0.126	0.126	0.126	0.126	0.126	0.126
0.100	0.164	0.166	0.180	0.181	0.206	0.184	0.164	0.192	0.248
0.200	0.174	0.176	0.191	0.196	0.223	0.204	0.174	0.208	0.267
0.250	0.178	0.180	0.196	0.201	0.230	0.214	0.178	0.214	0.273
0.300	0.181	0.182	0.200	0.205	0.237	0.222	0.181	0.219	0.279
0.400	0.187	0.187	0.210	0.214	0.252	0.238	0.187	0.230	0.302
0.500	0.195	0.193	0.219	0.225	0.266	0.253	0.193	0.243	0.326
0.600	0.203	0.201	0.229	0.242	0.283	0.272	0.201	0.258	0.354
0.700	0.213	0.212	0.246	0.265	0.308	0.299	0.212	0.278	0.389
0.800	0.234	0.230	0.269	0.314	0.366	0.350	0.230	0.312	0.436
0.850	0.253	0.252	0.291	0.351	0.422	0.399	0.252	0.343	0.486
0.900	0.285	0.305	0.331	0.428	0.511	0.480	0.285	0.404	0.624
0.925	0.327	0.359	0.370	0.516	0.601	0.554	0.327	0.471	0.737
0.930	0.338	0.374	0.386	0.540	0.624	0.581	0.338	0.490	0.761
0.950	0.391	0.454	0.482	0.702	0.764	0.698	0.391	0.600	0.913
0.960	0.431	0.529	0.556	0.798	0.853	0.759	0.431	0.671	1.013
0.975	0.518	0.784	0.717	1.084	1.188	0.922	0.518	0.876	1.337
0.980	0.566	0.871	0.823	1.278	1.353	0.997	0.566	0.985	1.533
0.990	0.744	1.194	1.315	1.783	1.854	1.269	0.744	1.364	2.181

Table 18. Cumulative Distributions of Zenith Atmospheric Attenuation at Ka-Band for Madrid DSCC, dB

CD	January	February	March	April	May	June
0.000	0.121	0.121	0.121	0.121	0.121	0.121
0.100	0.138	0.138	0.155	0.157	0.181	0.191
0.200	0.150	0.148	0.165	0.169	0.195	0.205
0.250	0.153	0.151	0.168	0.172	0.199	0.209
0.300	0.157	0.155	0.173	0.176	0.205	0.215
0.400	0.165	0.161	0.181	0.183	0.215	0.224
0.500	0.177	0.171	0.191	0.193	0.222	0.233
0.600	0.192	0.183	0.202	0.206	0.231	0.242
0.700	0.222	0.196	0.219	0.223	0.242	0.251
0.800	0.297	0.221	0.252	0.260	0.269	0.264
0.850	0.382	0.257	0.289	0.297	0.326	0.274
0.900	0.541	0.332	0.370	0.355	0.454	0.292
0.925	0.725	0.412	0.462	0.414	0.593	0.308
0.930	0.757	0.429	0.481	0.428	0.621	0.313
0.950	1.021	0.560	0.599	0.549	0.792	0.358
0.960	1.122	0.634	0.675	0.621	0.887	0.399
0.975	1.371	0.848	0.886	0.788	1.117	0.541
0.980	1.448	0.922	0.969	0.839	1.204	0.641
0.990	1.754	1.218	1.264	1.031	1.508	1.052

Table 18 (Cont'd). Cumulative Distributions of Zenith Atmospheric Attenuation at Ka-Band for Madrid DSCC, dB

CD	July	August	September	October	November	December	Minimum	Year Average	Maximum
0.000	0.121	0.121	0.121	0.121	0.121	0.121	0.121	0.121	0.121
0.100	0.201	0.202	0.190	0.171	0.119	0.138	0.119	0.165	0.202
0.200	0.213	0.215	0.206	0.194	0.152	0.152	0.148	0.180	0.215
0.250	0.217	0.219	0.211	0.201	0.157	0.157	0.151	0.184	0.219
0.300	0.222	0.226	0.218	0.211	0.166	0.166	0.155	0.191	0.226
0.400	0.231	0.234	0.230	0.227	0.176	0.180	0.161	0.200	0.234
0.500	0.238	0.242	0.241	0.244	0.188	0.194	0.171	0.211	0.244
0.600	0.246	0.251	0.254	0.263	0.205	0.213	0.183	0.224	0.263
0.700	0.254	0.260	0.266	0.290	0.228	0.246	0.196	0.241	0.290
0.800	0.263	0.272	0.282	0.353	0.272	0.322	0.221	0.277	0.353
0.850	0.269	0.279	0.293	0.427	0.340	0.406	0.257	0.319	0.427
0.900	0.279	0.290	0.314	0.568	0.478	0.549	0.279	0.401	0.568
0.925	0.286	0.297	0.338	0.714	0.627	0.687	0.286	0.486	0.725
0.930	0.287	0.299	0.343	0.742	0.651	0.707	0.287	0.501	0.757
0.950	0.298	0.310	0.391	0.958	0.857	0.879	0.298	0.624	1.021
0.960	0.305	0.320	0.440	1.061	0.947	0.962	0.305	0.689	1.122
0.975	0.330	0.350	0.606	1.325	1.190	1.187	0.330	0.864	1.371
0.980	0.351	0.372	0.736	1.438	1.257	1.259	0.351	0.938	1.448
0.990	0.460	0.468	1.253	1.896	1.532	1.520	0.460	1.225	1.896

Table 19. Monthly and Year-Average Rainfall Amounts at the DSN Antenna Locations

Month	Goldstone		Canberra		Madrid	
	inches	mm	inches	mm	inches	mm
January	1.02	25.9	3.61	91.7	1.48	37.5
February	1.18	30.0	2.74	69.7	1.38	35.0
March	0.90	22.9	2.90	73.6	1.10	28.0
April	0.20	5.1	2.85	72.4	1.87	47.5
May	0.19	4.8	2.94	74.8	1.56	39.5
June	0.04	1.0	2.70	68.7	1.26	32.0
July	0.35	8.9	3.36	85.3	0.57	14.5
August	0.59	15.0	3.90	99.0	0.59	15.0
September	0.39	9.9	3.73	94.7	1.16	29.5
October	0.15	3.8	3.70	94.0	1.54	39.0
November	0.23	5.8	3.50	88.8	2.01	51.0
December	0.57	14.5	2.42	61.4	1.75	44.5
Year Average	5.81	147.6	38.67	982.1	16.26	413.0

Table 20. Parameters for X-Band Planetary Noise Calculation, plus X-Band and Ka-Band Noise Temperatures at Mean Minimum Distance from Earth

Planet	Diameter (km)		Mean Distance from Earth (10^6 km)		Mean Distance from Sun		Blackbody Disk Temp (K)	T _{Planet} at Mean Minimum Distance (K)		
								X-Band		Ka-Band
	polar	equatorial	min.	max.	(10^6 km)	AU		70-m (74.4 dBi gain)	34-m (68.3 dBi gain)	34-m (78.8 dBi gain)
Mercury		4880	91.7	207.5	57.9	0.387	625	3.05	0.75	8.39
Venus		12104	41.4	257.8	108.2	0.723	490	72.10	17.70	198.58
Earth		12757	–	–	149.6	1.000	250–300 ¹	–	–	–
Mars		6794	78.3	377.5	227.9	1.523	180	2.33	0.57	6.43
Jupiter	134102	142984	628.7	927.9	778.3	5.203	152	13.53	3.32	37.27
Saturn	108728	120536	1279.8	1579.0	1429.4	9.555	155	2.37	0.58	6.52
Uranus		51118	2721.4	3020.6	2871.0	19.191	160	0.10	0.02	0.27
Neptune		49532	4354.4	4653.6	4504.0	30.107	160	0.04	0.01	0.10
Pluto		2274	5763.9	6063.1	5913.5	39.529	160	0.00	0.00	0.00

Note:

1. Ocean (250) and Land (300)